


Research Article

Robust Semisupervised Kernelized Fuzzy Local Information C-Means Clustering for Image Segmentation

Yao Yang ¹, Chengmao Wu,² Yawen Li,² and Shaoyu Zhang¹

¹School of Astronautics, Northwestern Polytechnical University, Xi'an, Shaanxi Province 710121, China

²School of Electronic Engineering, Xi'an University of Posts and Telecommunications, Xi'an, Shaanxi Province 710121, China

Correspondence should be addressed to Yao Yang; yangyao@nwpu.edu.cn

Received 17 November 2019; Accepted 11 January 2020; Published 23 March 2020

Academic Editor: Piotr Jędrzejowicz

Copyright © 2020 Yao Yang et al. This is an open access article distributed under the Creative Commons Attribution License, which permits unrestricted use, distribution, and reproduction in any medium, provided the original work is properly cited.

To improve the effectiveness and robustness of the existing semisupervised fuzzy clustering for segmenting image corrupted by noise, a kernel space semisupervised fuzzy C-means clustering segmentation algorithm combining utilizing neighborhood spatial gray information with fuzzy membership information is proposed in this paper. The mean intensity information of neighborhood window is embedded into the objective function of the existing semisupervised fuzzy C-means clustering, and the Lagrange multiplier method is used to obtain its iterative expression corresponding to the iterative solution of the optimization problem. Meanwhile, the local Gaussian kernel function is used to map the pixel samples from the Euclidean space to the high-dimensional feature space so that the cluster adaptability to different types of image segmentation is enhanced. Experiment results performed on different types of noisy images indicate that the proposed segmentation algorithm can achieve better segmentation performance than the existing typical robust fuzzy clustering algorithms and significantly enhance the antinoise performance.

1. Introduction

Fuzzy C-means (FCM) [1] is an unsupervised clustering method, which is widely used in numerous applications. In fact, it is an important tool in different fields, including data mining, machine learning, and image analysis. FCM has a simple iterative implementation procedure, fast convergence rate, and low storage requirements. However, it is a challenge to solve the image segmentation problem effectively through direct application of the existing FCM algorithm and clustering the pixels of the noisy images. Such a disadvantage is mainly because the existing FCM algorithm does not consider the high correlation between the current pixel and its neighborhood pixels. In order to solve this problem, Ahmed et al. [2] firstly proposed a robust FCM algorithm with spatial information constraint for medical image segmentation, but it has high time cost. Later, many researchers [3–7] proposed a series of improved fast robust FCM algorithms using local and nonlocal filtered information, sparse reconstruction information of neighborhood window. The shortcoming of these robust FCM algorithms is

that they cannot automatically determine spatial information constraint parameters. For this reason, Yang and Tsai [8] proposed a robust adaptive kernelized fuzzy clustering segmentation algorithm with spatial bias correction; its regularization constraint parameter is constructed by interclass separation measure. Wang et al. [9] put forward a robust fuzzy clustering segmentation algorithm with local and nonlocal spatial constraints; its weighted constraint parameter is constructed by Gaussian function of gray information deviation between current central pixel and its neighborhood pixels. In addition, the constraint parameter of robust fuzzy clustering with spatial constraint is constructed by variance or deviation of neighborhood pixels in literature [10–12]. Zhong et al. [13] gave an adaptive memetic fuzzy clustering with partition entropy for remote sensing image segmentation. These adaptive fuzzy clustering algorithms with spatial constraints greatly promote the rapid development of the robust fuzzy clustering segmentation theory, but their ability to suppress noise is weak. Considering that robust fuzzy clustering algorithm with spatial gray information constraints has a high computational time

cost, Chuang et al. [14] proposed a robust fuzzy clustering algorithm with spatial fuzzy membership degree information constraints. Adhikari et al. [15] also proposed a conditional spatial fuzzy clustering for medical MRI image segmentation. Their ability to suppress noise needs to be further enhanced. Cai et al. [16] also proposed a fast robust fuzzy clustering algorithm using linear weighted filtering image, and its disadvantage is that the image detail information may be lost in the segmentation results.

In many robust fuzzy clustering algorithms with fuzzy information constraints, Pham [17] firstly proposed a robust regularized fuzzy clustering segmentation algorithm, and its clustering objective function is embedded with neighborhood membership information. Later, Zhang and Yang et al. [18, 19] also improved a robust regularized fuzzy clustering algorithm with neighborhood membership constraints, but their shortcoming is that the parameter of local fuzzy information regularization item cannot be adaptively determined. Until 2010, Greek scholars Krinidis and Chatzis [20] proposed a new fuzzy local information clustering algorithm without adjusting parameter for noisy image segmentation, and it has attracted many scholars' attention. Li et al. [21] firstly gave an improved fuzzy local information clustering algorithm with edge weighting for edge preserving segmentation image. Gong et al. [22] presented a kernelized fuzzy weighted local information clustering algorithm, and it has stronger noise suppression ability than the robust segmentation algorithm in [21]. Later, many scholars [23–27] have discussed a series of improved fuzzy weighted local information clustering algorithms, and their main differences are reflected in the weighting coefficient construction methods of fuzzy local information. These researches greatly promote the development of fuzzy local information clustering algorithm, but their algorithms require high time cost, and are not entirely suitable for real-time segmentation of large-scale images.

Although robust fuzzy clustering algorithms with spatial gray information and fuzzy membership constraints enhance the ability to suppress noise or singular data, they still have some shortcomings, including the sensitivity to initial values and constraints in achieving local optimal solutions. Therefore, a group of scholars have proposed the application of bionic probability optimization methods, including the genetic algorithm (GA), to obtain approximate optimal clustering results. Moreover, others scholars have proposed a semisupervised fuzzy clustering algorithm (SSFCA) that uses partial prior information for clustering data samples to improve the performance of the unsupervised fuzzy clustering [28, 29]. Semisupervised fuzzy C-means clustering is a semisupervised improvement of the sample membership degree constraint based on the existing FCM algorithm. The application of clustering prior knowledge in the FCM algorithm is generally based on the modification of the clustering objective function [30–35] or the clustering process [36]. Based on modification of objective function, Pedrycz [30] proposed a semisupervised fuzzy clustering algorithm with the membership deviation. In his proposed algorithm, constraints are minimized by introducing the clustering process and an appropriate penalty function is

applied to promote the membership of the supervised information constraint to the known category. The semi-supervised fuzzy clustering algorithm has been successfully applied in the data analysis [37–39], shape annotation [40], remote sensing image segmentation [41, 42], and the image change detection [43]. Based on these studies, Pedrycz and Waletzky [44] multiplied the supervision information of the prior classification labels by a Boolean vector to distinguish whether the sample is supervised or not. Furthermore, they introduced a regular factor to compromise the proportion of the supervised and the unsupervised parts of the objective function and obtained an improved semisupervised FCM algorithm. Stutz and Runkler [45] explained the regular term factor as the credibility of the labelled samples to play the guiding role of the sample prior information on the clustering. Moreover, Bouchachia and Pedrycz [46] proposed a semisupervised FCM algorithm that can effectively deal with the problem that the number of samples is smaller than the number of clusters. Bouchachia and Pedrycz [31] proposed a semisupervised FCM algorithm based on the reproducing kernel Hilbert space. The above mentioned semisupervised FCM algorithms are based on the modification of objective function. They provide new ideas for the transition from the classical unsupervised mode clustering to the semi-supervised mode clustering. Not only does this transition improve performance of the existing FCM clustering, but also it can be applied in numerous fields such as the image segmentation, remote sensing image change detection, and the fault diagnosis. Recently, Tuan and Son et al. [47–50] adopted the semisupervised fuzzy clustering for complicated medical dental image segmentation and achieved great success in this regard. However, the algorithm is very complicated and requires artificial parameters selection when it is applied in the interactive image segmentation in complex situations. In order to enhance the robustness and effectiveness of the fuzzy clustering to solve complex image segmentation problems, some scholars combined the spatial gray and the fuzzy membership information with information of the current clustering pixels to expand the semisupervised fuzzy clustering idea and proposed new semisupervised fuzzy clustering segmentation algorithms [51]. Moreover, Chatzis et al. [52–56] utilized KL divergence to propose a series of improved semisupervised fuzzy clustering algorithm for adjusting the local information and the sample fuzzy membership degree. But the introduction of KL divergence leads to the problem that there is power operation existing in the calculation of membership, which results in high time cost. In addition, KL divergence based semisupervised fuzzy clustering is difficult to choose the regular parameters of KL divergence item effectively. In a few words, these efforts greatly promoted the rapid development of the semisupervised fuzzy clustering segmentation theory.

Based on the existing semisupervised FCM algorithm theory, this paper intends to use the prior information of the pixel classification in the neighborhood window to semi-supervise the fuzzy clustering [55, 56] and guide clustering in the presence of noise or insufficient data. The process approaches the optimal clustering solution by iterative method.

Meanwhile, the regular constraint term of local information is embedded in the clustering objective function of semisupervised fuzzy clustering, which is expected to improve the ability of the fuzzy clustering algorithm to suppress noise. Besides, consider utilizing the local Gaussian kernel function of the reproducing kernel Hilbert space to map pixel samples obtained from the European space to the high-dimensional feature space. Then, a semisupervised fuzzy local C-means clustering algorithm for the kernel space will be proposed to solve the problem of efficient classification of linearly inseparable sample sets in high-dimensional feature space. In order to evaluate the performance of the proposed algorithm, segmentation tests of different types of noisy image of synthetic, standard, medical, and remote sensing images are performed.

2. Semisupervised Fuzzy Clustering with Spatial Membership Constraints

In the conventional fuzzy C-means clustering algorithm for image segmentation, it is assumed that image pixels are independent of each other. In other words, without considering the influence of neighboring pixels on the current clustering pixels, the existing FCM algorithm is sensitive to noise. Therefore, the antinoise performance of the clustering segmentation algorithm should be improved. When the classification prior information of the current clustering pixel is known, embedding it into the objective function of fuzzy C-means clustering can enhance the clustering accuracy and suppress the noise influence on the clustering results. Bouchachia and Pedrycz [37] proposed a semisupervised FCM algorithm for improving fuzzy C-means clustering. He introduced the classification supervised fuzzy

information to the membership regularization term so that the corresponding fuzzy membership degree of the sample clustering is not far from the sample supervised fuzzy information, which is beneficial to the sample clustering. The objective function of semisupervised fuzzy clustering is mathematically expressed in the following form:

$$J_m(\mathbf{U}, \mathbf{V}) = \sum_{i=1}^n \sum_{k=1}^c u_{ik}^m d_{ik}^2 + \alpha \sum_{i=1}^n \sum_{k=1}^c (u_{ik} - b_i f_{ik})^m d_{ik}^2, \quad (1)$$

where u_{ik} ($i = 1, 2, \dots, n; k = 1, 2, \dots, c$) is the membership of the i -th sample in the j -th cluster and it is subject to the constraint $\sum_{k=1}^c u_{ik} = 1$. Moreover, $d_{ik}^2 = \|\mathbf{x}_i - \mathbf{v}_k\|^2$ denotes the Euclidean distance between sample \mathbf{x}_i and the cluster center \mathbf{v}_k . $m \in [1.5, 2.5]$, $\alpha \geq 0$, and f_{ik} are the fuzzy weight factor, which is a controlling factor for semisupervised learning items and the prior category supervised fuzzy information, respectively. Finally, b_i is the Boolean value indicating whether the sample is supervised or not. More specifically, when $b_i = 1$, the i -th sample is supervised information, while $b_i = 0$ indicates that the i -th sample is unsupervised.

For the objective function (1) of semisupervised fuzzy clustering, when the fuzzy factor $m \neq 2$, the membership degree u_{ik} and cluster center \mathbf{v}_k for the iterative solution of the problem cannot be obtained by a strict mathematical derivation. However, the foregoing equations can be analogized according to its iterative expression when $m = 2$. The corresponding iterative expression that can solve the optimization problem is obtained through the following equations:

$$u_{ik} = \frac{1}{1 + \alpha^{1/(m-1)}} \frac{1 + \alpha^{1/(m-1)} (1 - b_i \sum_{k=1}^c f_{ik})}{\sum_{r=1}^c \left(\|\mathbf{x}_i - \mathbf{v}_k\|^2 / \|\mathbf{x}_i - \mathbf{v}_r\|^2 \right)^{1/(m-1)}} + \frac{\alpha^{1/(m-1)}}{1 + \alpha^{1/(m-1)}} b_i f_{ik}, \quad (2)$$

$$\mathbf{v}_k = \frac{\sum_{i=1}^n \left[u_{ik}^m + \alpha \left((u_{ik} - b_i f_{ik})^2 \right)^{m/2} \right] \cdot \mathbf{x}_i}{\sum_{i=1}^n \left[u_{ik}^m + \alpha \left((u_{ik} - b_i f_{ik})^2 \right)^{m/2} \right]}. \quad (3)$$

It can be shown that equation (2) still satisfies the membership constraints $\sum_{k=1}^c u_{ik} = 1$ of the semisupervised fuzzy clustering. The construction idea of equations (2) and (3) is inspired by research work [57]. In particular, for equations (2) and (3), when fuzzy factor m is 2, then equations (2) and (3) degenerate into the iterative expression of existing semisupervised fuzzy clustering [28].

In our proposed method, when the semisupervised fuzzy clustering is applied on the image segmentation, f_{ik} is replaced with \bar{u}_{ik} , while $b_i = 1$. Under this circumstance, \bar{u}_{ik} represents the mean value of the fuzzy membership of the pixel neighborhood prior classification. The corresponding calculate expression is

$$\bar{u}_{ik} = \frac{1}{N_R} \sum_{r \in N_i} u_{rk}, \quad (4)$$

where N_i and N_R are a set of neighbors of all pixels in a neighborhood window centered on the first pixel and the number of pixels in the neighborhood window, respectively.

For the objective function (1), the fuzzy factor m is often set to 2. When the Lagrange multiplier method is utilized, the constraint optimization problem corresponding to equation (1) is transformed into an unconstrained optimization problem. For the transformed unconstrained optimization function, the membership degree u_{ik} and the cluster center \mathbf{v}_k are separately biased and set to zero, so the membership degree and the cluster center expression of the

iterative solution to the optimization problem can be obtained as follows:

$$u_{ik} = \frac{1}{1 + \alpha} \frac{1 + \alpha(1 - \sum_{k=1}^c \bar{u}_{ik})}{\sum_{r=1}^c \|\mathbf{x}_i - \mathbf{v}_k\|^2 / \|\mathbf{x}_i - \mathbf{v}_r\|^2} + \frac{\alpha}{1 + \alpha} \bar{u}_{ik}, \quad (5)$$

$$\mathbf{v}_k = \frac{\sum_{i=1}^n [u_{ik}^2 + \alpha(u_{ik} - \bar{u}_{ik})^2] \cdot \mathbf{x}_i}{\sum_{i=1}^n [u_{ik}^2 + \alpha(u_{ik} - \bar{u}_{ik})^2]}. \quad (6)$$

In short, equations (5) and (6) are a simple and closed-form solution for the robust semisupervised fuzzy clustering with $m=2$ for segmenting image with noise. Similarly, equations (5) and (6) can be used to obtain more universal semisupervised fuzzy local clustering image segmentation. The membership u_{ik} and the cluster center \mathbf{v}_k are expressed as

$$u_{ik} = \frac{1}{1 + \alpha^{1/(m-1)}} \frac{1 + \alpha^{1/(m-1)}(1 - \sum_{k=1}^c \bar{u}_{ik})}{\sum_{r=1}^c \left(\|\mathbf{x}_i - \mathbf{v}_k\|^2 / \|\mathbf{x}_i - \mathbf{v}_r\|^2 \right)^{1/(m-1)}} + \frac{\alpha^{1/(m-1)}}{1 + \alpha^{1/(m-1)}} \bar{u}_{ik}, \quad (7)$$

$$\mathbf{v}_k = \frac{\sum_{i=1}^n \left[u_{ik}^m + \alpha \left((u_{ik} - \bar{u}_{ik})^2 \right)^{m/2} \right] \cdot \mathbf{x}_i}{\sum_{i=1}^n \left[u_{ik}^m + \alpha \left((u_{ik} - \bar{u}_{ik})^2 \right)^{m/2} \right]}. \quad (8)$$

Considering the iterative solutions (7) and (8), a semi-supervised fuzzy C-means clustering (hereafter called the SSFCM) algorithm for image segmentation can be obtained.

Moreover, in the cluster center iterative expressions (6) and (8), $((u_{ik} - \bar{u}_{ik})^2)^{m/2}$ does not have to be expressed in form of $(u_{ik} - \bar{u}_{ik})^m$ because there may be negative values for the term $(u_{ik} - \bar{u}_{ik})^m$, resulting in the calculation of the cluster center away from the real cluster center. This problem should be eliminated from the semisupervised fuzzy clustering scheme through general fuzzy factor.

3. SSFCM Algorithm with Spatial Gray and Membership Information Constraints

The SSFCM algorithm utilizes the mean information \bar{u}_{ik} of the prior membership degree of the neighborhood pixel classification, which can reduce or even suppress the sensitivity of the clustering algorithm to the noise in the segmentation image. However, this method can only suppress the impact originating from very weak noise. In fact, it is necessary to enhance the noise suppression ability of the semisupervised fuzzy clustering segmentation algorithms to deal with the segmentation problem of images corrupted by strong noise. Therefore, the present study considers the neighborhood gray information of the current clustering pixels so that the image segmentation results can maintain reasonable regional consistency. Hence, the local neighbor

information of the pixel is embedded in the objective function of the SSFCM algorithm in the form of a constraint regular term. This term enhances the ability of the semi-supervised fuzzy clustering to suppress the influence of noise on segmentation results.

In order to improve the antinoise robustness of FCM algorithm, Ahmed et al. [2] proposed a robust FCM_S algorithm with spatial neighborhood information constraints of current clustering pixel; this algorithm can significantly improve the segmentation effect of images corrupted by noise. However, the algorithm requires the distance calculation from each pixel to its neighborhood pixels and the cluster center. Subsequently, the FCM_S algorithm has high time cost so that it is an inappropriate scheme for applications with high real-time requirements, including the intelligent transportation and the industrial automation detection. Therefore, Chen and Zhang [3] proposed the FCM_S1 algorithm to improve the conventional FCM_S algorithm from the view of computational speed. In the FCM_S1 algorithm, pixels in neighborhood window are replaced with mean value of pixel neighborhood. In the present study, it is intended to embed the FCM_S1 algorithm in the pixel neighborhood information constraint regular term. Furthermore, the regular term is added to the objective function of the SSFCM so that the objective function of SSFCM_S algorithm is defined as follows:

$$J_m(\mathbf{U}, \mathbf{V}) = \sum_{i=1}^n \sum_{k=1}^c u_{ik}^m \|\mathbf{x}_i - \mathbf{v}_k\|^2 + \tau \sum_{i=1}^n \sum_{k=1}^c u_{ik}^m \|\bar{\mathbf{x}}_i - \mathbf{v}_k\|^2 + \alpha \sum_{i=1}^n \sum_{k=1}^c (u_{ik} - \bar{u}_{ik})^m \|\mathbf{x}_i - \mathbf{v}_k\|^2 + \alpha \tau \sum_{i=1}^n \sum_{k=1}^c (u_{ik} - \bar{u}_{ik})^m \|\bar{\mathbf{x}}_i - \mathbf{v}_k\|^2, \quad (9)$$

where τ and $\bar{\mathbf{x}}_i$ are the control coefficient and the mean value of the gray information of the neighboring pixels, respectively. It should be indicated that $\bar{\mathbf{x}}_i$ is defined in the form below:

$$\bar{\mathbf{x}}_i = \frac{1}{N_R} \sum_{r \in N_i} \mathbf{x}_r. \quad (10)$$

For optimization problems of equation (9) of robust semisupervised fuzzy clustering with spatial gray

information and fuzzy membership constraints, its corresponding iterative equation of the membership degree u_{ik} and the cluster center \mathbf{v}_k can be constructed according to

$$u_{ik} = \frac{1}{1 + \alpha^{1/(m-1)}} \frac{1 + \alpha^{1/(m-1)} (1 - \sum_{k=1}^c \bar{u}_{ik})}{\sum_{r=1}^c \left(\left(\|\mathbf{x}_i - \mathbf{v}_k\|^2 + \tau \|\bar{\mathbf{x}}_i - \mathbf{v}_k\|^2 \right) / \left(\|\mathbf{x}_i - \mathbf{v}_r\|^2 + \tau \|\bar{\mathbf{x}}_i - \mathbf{v}_r\|^2 \right) \right)^{1/(m-1)}} + \frac{\alpha^{1/(m-1)}}{1 + \alpha^{1/(m-1)}} \bar{u}_{ik}, \quad (11)$$

$$\mathbf{v}_k = \frac{\sum_{i=1}^n \left[u_{ik}^m + \alpha \left((u_{ik} - \bar{u}_{ik})^2 \right)^{m/2} \right] \cdot (\mathbf{x}_i + \tau \cdot \bar{\mathbf{x}}_i)}{\sum_{i=1}^n \left[u_{ik}^m + \alpha \left((u_{ik} - \bar{u}_{ik})^2 \right)^{m/2} \right] \cdot (1 + \tau)}. \quad (12)$$

In short, equations (11) and (12) can be applied to solve the optimization problem of robust semisupervised fuzzy clustering with spatial neighborhood information constraint for image segmentation with certain universality.

It can be shown that the robust semisupervised fuzzy segmentation method based on equations (11) and (12) is convergent, and the proving method of the convergence of the existing FCM algorithm can be applied to prove the corresponding convergence of this proposed robust semisupervised fuzzy clustering.

4. Robust Semisupervised Kernel-Based Fuzzy Clustering Segmentation Method

The SSFCM_S algorithm with spatial gray and membership information constraints obtains reasonable antinoise performance when segmenting image corrupted by noise. In

equations (7) and (8), and their detailed descriptions are as follows:

order to improve the ability of the algorithm to cluster

nonconvex irregular data, pixel value is mapped from Euclidean space to high-dimensional feature space by nonlinear mapping. Then, semisupervised fuzzy clustering is performed on it. By kernelizing the Euclidean distance in the objective function of the SSFCM_S algorithm, a new semisupervised fuzzy local information C-means image segmentation algorithm is obtained, which is based on spatial neighborhood information constraints. This algorithm is named semisupervised kernel-based fuzzy C-means clustering with spatial gray and membership constraints for image segmentation, abbreviated as KSSFCM_S algorithm. The improved objective function of KSSFCM_S algorithm is presented as follows:

$$J_m(\mathbf{U}, \mathbf{V}) = \sum_{i=1}^n \sum_{k=1}^c u_{ik}^m \|\Phi(\mathbf{x}_i) - \Phi(\mathbf{v}_k)\|^2 + \tau \sum_{i=1}^n \sum_{k=1}^c u_{ik}^m \|\Phi(\bar{\mathbf{x}}_i) - \Phi(\mathbf{v}_k)\|^2 + \alpha \sum_{i=1}^n \sum_{k=1}^c (u_{ik} - \bar{u}_{ik})^m \|\Phi(\mathbf{x}_i) - \Phi(\mathbf{v}_k)\|^2 + \alpha \tau \sum_{i=1}^n \sum_{k=1}^c (u_{ik} - \bar{u}_{ik})^m \|\Phi(\bar{\mathbf{x}}_i) - \Phi(\mathbf{v}_k)\|^2, \quad (13)$$

where Φ is a nonlinear mapping, which maps data samples from low-dimensional Euclidean space to high-dimensional reproducing kernel Hilbert space. According to the characteristics of the kernel function in the reproducing kernel Hilbert space, the following expression is obtained:

$$\begin{aligned} \|\Phi(\mathbf{x}_i) - \Phi(\mathbf{v}_k)\|^2 &= [\Phi(\mathbf{x}_i) - \Phi(\mathbf{v}_k)]^T [\Phi(\mathbf{x}_i) - \Phi(\mathbf{v}_k)] \\ &= K(\mathbf{x}_i, \mathbf{x}_i) - 2K(\mathbf{x}_i, \mathbf{v}_k) + K(\mathbf{v}_k, \mathbf{v}_k). \end{aligned} \quad (14)$$

The Gaussian kernel function that meets the Mercer condition is applied as follows:

$$K(\mathbf{x}_i, \mathbf{v}_k) = \exp\left(-\frac{\|\mathbf{x}_i - \mathbf{v}_k\|^2}{2\sigma^2}\right). \quad (15)$$

Therefore,

$$\|\Phi(\mathbf{x}_i) - \Phi(\mathbf{v}_k)\|^2 = 2 - 2 \exp\left(-\frac{\|\mathbf{x}_i - \mathbf{v}_k\|^2}{2\sigma^2}\right), \quad (16)$$

where σ is the scale parameter, whose value is the key to the performance of the image segmentation. The scale parameter σ can be determined by applying the principle of distance standard deviation between samples:

$$\sigma = \left(\frac{1}{n-1} \sum_{i=1}^n (d_i - \bar{d})^2 \right)^{1/2}, \quad (17)$$

where $d_i = \|\mathbf{x}_i - \bar{\mathbf{x}}\|$ is the distance of the pixel value \mathbf{x}_i from mean value $\bar{\mathbf{x}}$ of all pixels. Moreover, \bar{d} is the mean value of the corresponding distance d_i from all pixel points. The

expressions of the pixel center \bar{x} and the distance mean \bar{d} are represented as follows:

$$\bar{x} = \frac{1}{n} \sum_{i=1}^n \mathbf{x}_i, \bar{d} = \frac{1}{n} \sum_{i=1}^n \mathbf{d}_i. \quad (18)$$

Considering the clustering objective function (13), if $m = 2$ is selected to obtain a simple and closed-form solution, the Lagrange multiplier method can be used to obtain the expression of the membership degree u_{ik} of the optimization problem corresponding to the objective function as follows:

$$u_{ik} = \frac{1}{1 + \alpha} \frac{1 + \alpha(1 - \sum_{k=1}^c \bar{u}_{ik})}{\sum_{r=1}^c D(\mathbf{x}_i, \mathbf{v}_k)/D(\mathbf{x}_i, \mathbf{v}_r)} + \frac{\alpha}{1 + \alpha} \bar{u}_{ik}, \quad (19)$$

where

$$\begin{aligned} D(\mathbf{x}_i, \mathbf{v}_k) &= \|\Phi(\mathbf{x}_i) - \Phi(\mathbf{v}_k)\|^2 + \tau \|\Phi(\bar{\mathbf{x}}_i) - \Phi(\mathbf{v}_k)\|^2 \\ &= 2(1 + \tau) - 2(K(\mathbf{x}_i, \mathbf{v}_k) + K(\bar{\mathbf{x}}_i, \mathbf{v}_k)) \\ &= 2(1 + \tau) - 2 \left(\exp\left(-\frac{\|\mathbf{x}_i - \mathbf{v}_k\|^2}{2\sigma^2}\right) \right. \\ &\quad \left. + \tau \exp\left(-\frac{\|\bar{\mathbf{x}}_i - \mathbf{v}_k\|^2}{2\sigma^2}\right) \right). \end{aligned} \quad (20)$$

Furthermore, the expression of the cluster center \mathbf{v}_k can be obtained as

$$\mathbf{v}_k = \frac{\sum_{i=1}^n \left[u_{ik}^2 + \alpha(u_{ik} - \bar{u}_{ik})^2 \right] \cdot (K(\mathbf{x}_i, \mathbf{v}_k)\mathbf{x}_i + \tau \cdot K(\mathbf{x}_i, \mathbf{v}_k)\bar{\mathbf{x}}_i)}{\sum_{i=1}^n \left[u_{ik}^2 + \alpha(u_{ik} - \bar{u}_{ik})^2 \right] \cdot (K(\mathbf{x}_i, \mathbf{v}_k) + \tau \cdot K(\mathbf{x}_i, \mathbf{v}_k))}, \quad (21)$$

where $K_1 = K(\mathbf{x}_i, \mathbf{v}_k)$ and $K_2 = K(\bar{\mathbf{x}}_i, \mathbf{v}_k)$.

Similarly, an iterative solution expression with $m \neq 2$ that can be extended by equations (19) and (21) is described as follows:

$$u_{ik} = \frac{1}{1 + \alpha^{1/(m-1)}} \frac{1 + \alpha^{1/(m-1)}(1 - \sum_{k=1}^c \bar{u}_{ik})}{\sum_{r=1}^c (D(\mathbf{x}_i, \mathbf{v}_k)/D(\mathbf{x}_i, \mathbf{v}_r))^{1/(m-1)}} + \frac{\alpha^{1/(m-1)}}{1 + \alpha^{1/(m-1)}} \bar{u}_{ik}, \quad (22)$$

$$\mathbf{v}_k = \frac{\sum_{i=1}^n \left[u_{ik}^m + \alpha((u_{ik} - \bar{u}_{ik})^2)^{m/2} \right] \cdot (K(\mathbf{x}_i, \mathbf{v}_k)\mathbf{x}_i + \tau \cdot K(\mathbf{x}_i, \mathbf{v}_k)\bar{\mathbf{x}}_i)}{\sum_{i=1}^n \left[u_{ik}^m + \alpha((u_{ik} - \bar{u}_{ik})^2)^{m/2} \right] \cdot (K(\mathbf{x}_i, \mathbf{v}_k) + \tau \cdot K(\mathbf{x}_i, \mathbf{v}_k))}. \quad (23)$$

Therefore, using equations (22) and (23), a semi-supervised fuzzy local C-means clustering algorithm is obtained based on the pixel neighborhood gray and membership information constraints in kernel space. The detailed algorithm is described as follows.

Step 1: read the grayscale image, initialize the number of iterations $t = 0$, choose fuzzy weight factor m , set the iteration termination condition $\varepsilon = 0.0001$, and the maximum number of iterations $\max T$.

Step 2: set the number of clusters c , the pixel neighborhood window size N_R , the semisupervised information item control parameter α , and spatial neighborhood information control parameter τ .

Step 3: the FCM algorithm is used to presegment the image. After the iteration of the FCM algorithm, the pixel clustering center \mathbf{v}_k ($1 \leq k \leq c$) and the membership matrix $\{u_{ik}\}$ are obtained, which are used as the initial clustering center $\mathbf{v}_k^{(0)}$ ($1 \leq k \leq c$) and initial membership matrix $\{u_{ik}^{(0)}\}$ of the KSSFCM_S algorithm, respectively.

Step 4: calculate the kernel distances $\|\Phi(\mathbf{x}_i) - \Phi(\mathbf{v}_k^{(t)})\|^2$ and $\|\Phi(\bar{\mathbf{x}}_i) - \Phi(\mathbf{v}_k^{(t)})\|^2$.

Step 5: calculate the prior fuzzy membership degree $\bar{\mathbf{U}}^{(t)} = \{\bar{u}_{ik}^{(t)}\}$ according to equation (4).

Step 6: calculate the update pixel cluster membership degree u_{ik} according to equation (22):

$$\begin{aligned} u_{ik}^{(t+1)} &= \frac{1}{1 + \alpha^{1/(m-1)}} \frac{1 + \alpha^{1/(m-1)}(1 - \sum_{k=1}^c \bar{u}_{ik}^{(t)})}{\sum_{r=1}^c (D(\mathbf{x}_i, \mathbf{v}_k^{(t)})/D(\mathbf{x}_i, \mathbf{v}_r^{(t)}))^{1/(m-1)}} \\ &\quad + \frac{\alpha^{1/(m-1)}}{1 + \alpha^{1/(m-1)}} \bar{u}_{ik}^{(t)}. \end{aligned} \quad (24)$$

Step 7: Calculate the update cluster center \mathbf{v}_k ($1 \leq k \leq c$) according to equation (23):

$$\mathbf{v}_k^{(t+1)} = \frac{\sum_{i=1}^n \left[(u_{ik}^{(t)})^m + \alpha((u_{ik}^{(t)} - \bar{u}_{ik}^{(t)})^2)^{m/2} \right] \cdot (K(\mathbf{x}_i, \mathbf{v}_k^{(t)})\mathbf{x}_i + \tau \cdot K(\mathbf{x}_i, \mathbf{v}_k^{(t)})\bar{\mathbf{x}}_i)}{\sum_{i=1}^n \left[(u_{ik}^{(t)})^m + \alpha((u_{ik}^{(t)} - \bar{u}_{ik}^{(t)})^2)^{m/2} \right] \cdot (K(\mathbf{x}_i, \mathbf{v}_k^{(t)}) + \tau \cdot K(\mathbf{x}_i, \mathbf{v}_k^{(t)}))}. \quad (25)$$

Step 8: update $t = t + 1$, if $\|\mathbf{V}^{(t)} - \mathbf{V}^{(t+1)}\| \leq \varepsilon$ or $t > \max T$, go to step 9; otherwise go to step 5 to execute.

Step 9: using the principle of the maximum membership of the sample classification $k^* = \arg \max_k \{u_{ik}\}$ ($1 \leq k \leq c$), classify and label each pixel in the image and obtain segmentation result.

5. Convergence Analysis of Robust Semisupervised Fuzzy in Kernel Space

The optimization model of robust semisupervised kernel-based fuzzy clustering with fuzzy weight factor $m = 2$ is described as follows:

$$J_m(\mathbf{U}, \mathbf{V}) = \sum_{i=1}^n \sum_{k=1}^c u_{ik}^2 \left[\|\Phi(\mathbf{x}_i) - \Phi(\mathbf{v}_k)\|^2 + \tau \|\Phi(\bar{\mathbf{x}}_i) - \Phi(\mathbf{v}_k)\|^2 \right] + \alpha \sum_{i=1}^n \sum_{k=1}^c (u_{ik} - \bar{u}_{ik})^2 \left[\|\Phi(\mathbf{x}_i) - \Phi(\mathbf{v}_k)\|^2 + \tau \|\Phi(\bar{\mathbf{x}}_i) - \Phi(\mathbf{v}_k)\|^2 \right], \quad (26)$$

s.t.

- (1) $u_{ik} \in [0, 1], i = 1, 2, \dots, n; j = 1, 2, \dots, c;$
- (2) $\sum_{k=1}^c u_{ik} = 1, i = 1, 2, \dots, n;$
- (3) $0 < \sum_{i=1}^n u_{ik} < n, k = 1, 2, \dots, c.$

The abovementioned constraint optimization expression (26) is transformed into an unconstrained optimization problem by the Lagrange multiplier method, and the corresponding optimization objective function is presented as follows:

$$L(\mathbf{U}, \mathbf{V}, \boldsymbol{\lambda}) = \sum_{i=1}^n \sum_{k=1}^c u_{ik}^2 \left[\|\Phi(\mathbf{x}_i) - \Phi(\mathbf{v}_k)\|^2 + \tau \|\Phi(\bar{\mathbf{x}}_i) - \Phi(\mathbf{v}_k)\|^2 \right] + \alpha \sum_{i=1}^n \sum_{k=1}^c (u_{ik} - \bar{u}_{ik})^2 \left[\|\Phi(\mathbf{x}_i) - \Phi(\mathbf{v}_k)\|^2 + \tau \|\Phi(\bar{\mathbf{x}}_i) - \Phi(\mathbf{v}_k)\|^2 \right] + \sum_{i=1}^n \lambda_i \left(1 - \sum_{k=1}^c u_{ik} \right). \quad (27)$$

Since the iterative algorithm of unconstrained optimization equation (27) is convergent, the present study utilizes the following Zangwill theorem [58] to prove that the proposed algorithm satisfies the convergence condition.

5.1. Zangwill Theorem. Let \mathbf{V} be the distance space, point $z^{(1)} \in \mathbf{V}$, $A: \mathbf{V} \rightarrow P(\mathbf{V})$ be the point-to-set mapping on \mathbf{V} . Then, the algorithm defined by A will generate the sequence $\{z^{(k)}\}_{k=1,2,\dots}$ with $z^{(1)}$ as the initial point; let $\Omega \subset \mathbf{V}$ be the solution set, if

- (1) All points $z^{(k)}$ belong to the tight subset of \mathbf{V} .
- (2) There is a continuous function $J: \mathbf{V} \rightarrow R$: (1) if $z \notin \Omega$, then for any $y \in A(z)$, there is $J(y) < J(z)$; (2) if $z \in \Omega$, the operator terminates, or for any $y \in A(z)$, there is $J(y) < J(z)$.
- (3) $z \notin \Omega$, mapping A is closed at point z ; then the algorithm terminates at the limit of a solution or any convergent subsequence is a solution.

Moreover, if the kernel space semisupervised fuzzy clustering iterative algorithm is convergent, the three conditions of the Zangwill theorem should be satisfied in [59], where the first condition of $L(\mathbf{U}, \mathbf{V}, \boldsymbol{\lambda})$ is the descending function.

Given the clustering center \mathbf{V} , the corresponding Lagrange function is described as follows:

$$L(\mathbf{U}, \boldsymbol{\lambda}) = \sum_{i=1}^n \sum_{k=1}^c u_{ik}^2 \left[\|\Phi(\mathbf{x}_i) - \Phi(\mathbf{v}_k)\|^2 + \tau \|\Phi(\bar{\mathbf{x}}_i) - \Phi(\mathbf{v}_k)\|^2 \right] + \alpha \sum_{i=1}^n \sum_{k=1}^c (u_{ik} - \bar{u}_{ik})^2 \left[\|\Phi(\mathbf{x}_i) - \Phi(\mathbf{v}_k)\|^2 + \tau \|\Phi(\bar{\mathbf{x}}_i) - \Phi(\mathbf{v}_k)\|^2 \right] + \sum_{i=1}^n \lambda_i \left(1 - \sum_{k=1}^c u_{ik} \right). \quad (28)$$

If $(\mathbf{U}^*, \boldsymbol{\lambda}^*)$ is the minimum point of the L function, then there are $\partial L(\mathbf{U}, \boldsymbol{\lambda}) / \partial u_{ik} |_{\mathbf{U}=\mathbf{U}^*} = 0$ and $\partial L(\mathbf{U}, \boldsymbol{\lambda}) / \partial \lambda_i |_{\boldsymbol{\lambda}=\boldsymbol{\lambda}^*} = 0$ so as to obtain

$$u_{ik}^* = \frac{1}{1 + \alpha} \frac{1 + \alpha (1 - \sum_{k=1}^c \bar{u}_{ik})}{\sum_{r=1}^c \left(\|\Phi(\mathbf{x}_i) - \Phi(\mathbf{v}_k)\|^2 + \tau \|\Phi(\bar{\mathbf{x}}_i) - \Phi(\mathbf{v}_k)\|^2 \right) / \left(\|\Phi(\mathbf{x}_i) - \Phi(\mathbf{v}_r)\|^2 + \tau \|\Phi(\bar{\mathbf{x}}_i) - \Phi(\mathbf{v}_r)\|^2 \right)} + \frac{\alpha}{1 + \alpha} \bar{u}_{ik}. \quad (29)$$

Therefore, $(\mathbf{U}^*, \boldsymbol{\lambda}^*)$ satisfies its necessary conditions.

In order to prove the sufficiency, it is necessary to consider the Hessian matrix of function $L(\mathbf{U}, \boldsymbol{\lambda})$ with size $nc \times nc$ at $\mathbf{U} = \mathbf{U}^*$:

$$\frac{\partial}{\partial u_{ab}} \left(\frac{\partial L(\mathbf{U}^*, \boldsymbol{\lambda}^*)}{\partial u_{ik}} \right) = \begin{cases} 0, & a \neq i, b \neq k, \\ 2(1 + \alpha) \left[\|\Phi(\mathbf{x}_i) - \Phi(\mathbf{v}_k)\|^2 + \tau \|\Phi(\bar{\mathbf{x}}_i) - \Phi(\mathbf{v}_k)\|^2 \right], & a = i, b = k. \end{cases} \quad (30)$$

The elements on the diagonal of the matrix are greater than 0, while the nondiagonal linear elements are 0. Therefore, the matrix can be determined to be positive definite, further indicating that $(\mathbf{U}^*, \boldsymbol{\lambda}^*)$ is the local minimum point of $L(\mathbf{U}, \boldsymbol{\lambda})$.

Given the fuzzy partition \mathbf{U} corresponding to the data sample $\{x_i, i = 1, 2, \dots, n\}$, the objective function corresponding to the cluster center \mathbf{V} is presented as follows:

$$\begin{aligned} L(\mathbf{V}) &= \sum_{i=1}^n \sum_{k=1}^c u_{ik}^2 \left[\|\Phi(\mathbf{x}_i) - \Phi(\mathbf{v}_k)\|^2 + \tau \|\Phi(\bar{\mathbf{x}}_i) - \Phi(\mathbf{v}_k)\|^2 \right] \\ &+ \alpha \sum_{i=1}^n \sum_{k=1}^c (u_{ik} - \bar{u}_{ik})^2 \left[\|\Phi(\mathbf{x}_i) - \Phi(\mathbf{v}_k)\|^2 \right. \\ &\left. + \tau \|\Phi(\bar{\mathbf{x}}_i) - \Phi(\mathbf{v}_k)\|^2 \right] + \sum_{i=1}^n \lambda_i \left(1 - \sum_{k=1}^c u_{ik} \right). \end{aligned} \quad (31)$$

If \mathbf{V}^* is the minimum point of $L(\mathbf{V})$, let $\partial L(\mathbf{V})/\partial \Phi(\mathbf{v}_j)|_{\mathbf{V}=\mathbf{V}^*} = 0$. Then,

$$\Phi(\mathbf{v}_k^*) = \frac{\sum_{i=1}^n [u_{ik}^2 + \alpha(u_{ik} - \bar{u}_{ik})^2] \Phi(\mathbf{x}_i) + \tau \Phi(\bar{\mathbf{x}}_i)}{\sum_{i=1}^n [u_{ik}^2 + \alpha(u_{ik} - \bar{u}_{ik})^2]}. \quad (32)$$

Furthermore, there can be

$$\begin{aligned} K(\mathbf{x}_i, \mathbf{v}_k^*) &= \frac{\sum_{l=1}^n [u_{lk}^2 + \alpha(u_{lk} - \bar{u}_{lk})^2] (K(\mathbf{x}_i, \mathbf{x}_l) + \tau K(\bar{\mathbf{x}}_i, \mathbf{x}_l))}{\sum_{l=1}^n [u_{lk}^2 + \alpha(u_{lk} - \bar{u}_{lk})^2]}, \\ K(\bar{\mathbf{x}}_i, \mathbf{v}_k^*) &= \frac{\sum_{l=1}^n [u_{lk}^2 + \alpha(u_{lk} - \bar{u}_{lk})^2] (K(\mathbf{x}_l, \bar{\mathbf{x}}_i) + \tau K(\bar{\mathbf{x}}_l, \bar{\mathbf{x}}_i))}{\sum_{l=1}^n [u_{lk}^2 + \alpha(u_{lk} - \bar{u}_{lk})^2]}. \end{aligned} \quad (33)$$

If the kernel function $K(\mathbf{x}, \mathbf{y}) = \exp(-(\|\mathbf{x} - \mathbf{y}\|^2/2\sigma^2))$, then let $\partial L(\mathbf{V})/\partial \mathbf{v}_j|_{\mathbf{V}=\mathbf{V}^*} = 0$, and the expression of clustering center \mathbf{v}_k^* is obtained as follows:

$$\begin{aligned} \mathbf{v}_k^* &= \frac{\sum_{l=1}^n [u_{lk}^2 + \alpha(u_{lk} - \bar{u}_{lk})^2] (K(\mathbf{x}_l, \mathbf{v}_k^*) \mathbf{x}_l + \tau K(\bar{\mathbf{x}}_l, \mathbf{v}_k^*) \bar{\mathbf{x}}_l)}{\sum_{l=1}^n [u_{lk}^2 + \alpha(u_{lk} - \bar{u}_{lk})^2]} \\ &= \frac{\sum_{l=1}^n \sum_{r=1}^n [u_{lk}^2 + \alpha(u_{lk} - \bar{u}_{lk})^2] [u_{rk}^2 + \alpha(u_{rk} - \bar{u}_{rk})^2] K(\mathbf{x}_l, \mathbf{x}_r) \mathbf{x}_l}{\left(\sum_{l=1}^n [u_{lk}^2 + \alpha(u_{lk} - \bar{u}_{lk})^2] \right)^2} \\ &+ \tau \frac{\sum_{l=1}^n \sum_{r=1}^n [u_{lk}^2 + \alpha(u_{lk} - \bar{u}_{lk})^2] [u_{rk}^2 + \alpha(u_{rk} - \bar{u}_{rk})^2] K(\bar{\mathbf{x}}_l, \mathbf{x}_r) \mathbf{x}_l}{\left(\sum_{l=1}^n [u_{lk}^2 + \alpha(u_{lk} - \bar{u}_{lk})^2] \right)^2} \\ &+ \tau \frac{\sum_{l=1}^n \sum_{r=1}^n [u_{lk}^2 + \alpha(u_{lk} - \bar{u}_{lk})^2] [u_{rk}^2 + \alpha(u_{rk} - \bar{u}_{rk})^2] K(\mathbf{x}_l, \bar{\mathbf{x}}_r) \bar{\mathbf{x}}_l}{\left(\sum_{l=1}^n [u_{lk}^2 + \alpha(u_{lk} - \bar{u}_{lk})^2] \right)^2} \\ &+ \tau^2 \frac{\sum_{l=1}^n \sum_{r=1}^n [u_{lk}^2 + \alpha(u_{lk} - \bar{u}_{lk})^2] [u_{rk}^2 + \alpha(u_{rk} - \bar{u}_{rk})^2] K(\bar{\mathbf{x}}_l, \bar{\mathbf{x}}_r) \bar{\mathbf{x}}_l}{\left(\sum_{l=1}^n [u_{lk}^2 + \alpha(u_{lk} - \bar{u}_{lk})^2] \right)^2}. \end{aligned} \quad (34)$$

Therefore, \mathbf{V}^* satisfies its necessary conditions.

$\partial L(\mathbf{V})/\partial \mathbf{v}_k$ is obtained initially as the follows:

In order to prove the sufficiency, it is required to consider the Hessian matrix of function $L(\mathbf{V})$ with size $c \times c$ at $\mathbf{V} = \mathbf{V}^*$.

$$\begin{aligned}
\frac{\partial L(\mathbf{V})}{\partial \mathbf{v}_k} &= -\frac{1}{\sigma^2} \sum_{i=1}^n \left[u_{ik}^2 + \alpha(u_{ik} - \bar{u}_{ik})^2 \right] \left[K(\mathbf{x}_i, \mathbf{v}_k)(\mathbf{x}_i - \mathbf{v}_k) + \tau K(\bar{\mathbf{x}}_i, \mathbf{v}_k)(\bar{\mathbf{x}}_i - \mathbf{v}_k) \right] \\
&= -\frac{1}{\sigma^2} \frac{\sum_{i=1}^n \sum_{r=1}^n \left[u_{ik}^2 + \alpha(u_{ik} - \bar{u}_{ik})^2 \right] \left[u_{rk}^2 + \alpha(u_{rk} - \bar{u}_{rk})^2 \right] K(\mathbf{x}_i, \mathbf{x}_r)(\mathbf{x}_i - \mathbf{v}_k)}{\sum_{r=1}^n \left[u_{rk}^2 + \alpha(u_{rk} - \bar{u}_{rk})^2 \right]} \\
&\quad - \frac{\tau}{\sigma^2} \frac{\sum_{i=1}^n \sum_{r=1}^n \left[u_{ik}^2 + \alpha(u_{ik} - \bar{u}_{ik})^2 \right] \left[u_{rk}^2 + \alpha(u_{rk} - \bar{u}_{rk})^2 \right] K(\bar{\mathbf{x}}_i, \mathbf{x}_r)(\mathbf{x}_i - \mathbf{v}_k)}{\sum_{r=1}^n \left[u_{rk}^2 + \alpha(u_{rk} - \bar{u}_{rk})^2 \right]} \\
&\quad - \frac{\tau}{\sigma^2} \frac{\sum_{i=1}^n \sum_{r=1}^n \left[u_{ik}^2 + \alpha(u_{ik} - \bar{u}_{ik})^2 \right] \left[u_{rk}^2 + \alpha(u_{rk} - \bar{u}_{rk})^2 \right] K(\bar{\mathbf{x}}_i, \mathbf{x}_r)(\bar{\mathbf{x}}_i - \mathbf{v}_k)}{\sum_{r=1}^n \left[u_{rk}^2 + \alpha(u_{rk} - \bar{u}_{rk})^2 \right]} \\
&\quad - \frac{\tau^2}{\sigma^2} \frac{\sum_{i=1}^n \sum_{r=1}^n \left[u_{ik}^2 + \alpha(u_{ik} - \bar{u}_{ik})^2 \right] \left[u_{rk}^2 + \alpha(u_{rk} - \bar{u}_{rk})^2 \right] K(\bar{\mathbf{x}}_i, \bar{\mathbf{x}}_r)(\bar{\mathbf{x}}_i - \mathbf{v}_k)}{\sum_{r=1}^n \left[u_{rk}^2 + \alpha(u_{rk} - \bar{u}_{rk})^2 \right]}.
\end{aligned} \tag{35}$$

Therefore, $\partial/\partial \mathbf{v}_j (\partial L(\mathbf{V})/\partial \mathbf{v}_k) = \begin{cases} 0, j \neq k \\ h(\mathbf{U}), j = k \end{cases}$ can be obtained, where

$$\begin{aligned}
h(\mathbf{U}) &= \frac{1}{\sigma^2} \frac{\sum_{i=1}^n \sum_{r=1}^n \left[u_{ik}^2 + \alpha(u_{ik} - \bar{u}_{ik})^2 \right] \left[u_{rk}^2 + \alpha(u_{rk} - \bar{u}_{rk})^2 \right] K(\mathbf{x}_i, \mathbf{x}_r)}{\sum_{r=1}^n \left[u_{rk}^2 + \alpha(u_{rk} - \bar{u}_{rk})^2 \right]} \\
&\quad + \frac{\tau}{\sigma^2} \frac{\sum_{i=1}^n \sum_{r=1}^n \left[u_{ik}^2 + \alpha(u_{ik} - \bar{u}_{ik})^2 \right] \left[u_{rk}^2 + \alpha(u_{rk} - \bar{u}_{rk})^2 \right] K(\bar{\mathbf{x}}_i, \mathbf{x}_r)}{\sum_{r=1}^n \left[u_{rk}^2 + \alpha(u_{rk} - \bar{u}_{rk})^2 \right]} \\
&\quad + \frac{\tau}{\sigma^2} \frac{\sum_{i=1}^n \sum_{r=1}^n \left[u_{ik}^2 + \alpha(u_{ik} - \bar{u}_{ik})^2 \right] \left[u_{rk}^2 + \alpha(u_{rk} - \bar{u}_{rk})^2 \right] K(\bar{\mathbf{x}}_i, \mathbf{x}_r)}{\sum_{r=1}^n \left[u_{rk}^2 + \alpha(u_{rk} - \bar{u}_{rk})^2 \right]} \\
&\quad + \frac{\tau^2}{\sigma^2} \frac{\sum_{i=1}^n \sum_{r=1}^n \left[u_{ik}^2 + \alpha(u_{ik} - \bar{u}_{ik})^2 \right] \left[u_{rk}^2 + \alpha(u_{rk} - \bar{u}_{rk})^2 \right] K(\bar{\mathbf{x}}_i, \bar{\mathbf{x}}_r)}{\sum_{r=1}^n \left[u_{rk}^2 + \alpha(u_{rk} - \bar{u}_{rk})^2 \right]}.
\end{aligned} \tag{36}$$

Obviously, $h(\mathbf{U}) > 0$ is established.

The elements on the diagonal of the Hessian matrix are greater than 0, and the nondiagonal linear elements are 0. Therefore, the matrix can be determined to be a positive definite, further indicating that \mathbf{V}^* is the local minimum point of $L(\mathbf{V})$.

The abovementioned analysis indicates that the kernel space semisupervised fuzzy local C-means clustering segmentation algorithm based on pixel neighborhood spatial information constraint is convergent.

6. Test Results and Analysis

In order to objectively and quantitatively analyze the anti-noise robust performance of different robust fuzzy clustering algorithm for segmentation image corrupted by noise, the present study evaluates the modified peak signal-to-noise ratio (PSNR) of the image quality as follows, which is used to evaluate the ability of suppressing noise for segmentation algorithm:

$$\text{PSNR} = 10 \cdot \log_{10} \left(\frac{255^2}{\text{MSE}} \right), \quad (37)$$

where $\text{MSE} = 1/l \times m \sum_{a=1}^l \sum_{b=1}^m \|I_{a,b} - K_{a,b}\|^2$ and the image size is $l \times m$. Moreover, $I_{a,b}$ and $K_{a,b}$ represent the ideal segmentation result for noise-free images and the actual segmentation result of the image corrupted by noise. It should be indicated that the larger the PSNR value is, the stronger the antinoise ability of segmentation algorithm can be.

Furthermore, in order to quantitatively evaluate the segmentation performance of the segmentation algorithm, the segmentation accuracy rate (SA) is defined as follows:

$$\text{SA} = \frac{\sum_{j=1}^c \frac{A_j \cap C_j}{\sum_{k=1}^c C_k}}{c}, \quad (38)$$

where c , A_j , and C_j represent the number of clustering classification categories, the number of pixels belonging to the j -th class by clustering by some algorithm, and the number of pixels in the image originally belonging to the j -th class, that is, the ideal true value, respectively. The higher the SA value is, the more consistent the actual segmentation result is with the ideal segmentation result, that is, the better the segmentation effect is; otherwise, the segmentation effect is poor.

6.1. Selection of Parameters α . The value of the semi-supervised fuzzy clustering regular term control parameter α is discussed in this section. Figure 1(a) shows that a Gaussian noise with mean value of 0 and mean square variance of 57 is added to the Lena image with the size of 512×512 to obtain noisy image shown in Figure 1(b). Moreover, Figure 2(a) shows that a salt-and-pepper noise with the intensity of 30% is added to the photographer image with the size of 256×256 to obtain a noisy image shown in Figure 2(b). Then, the two noisy images are segmented by using the KSSFCM_S algorithm proposed in this study. It should be indicated that parameter α is assigned as 10 to 15, respectively. Moreover, Figures 1 and 2 only show the segmentation results when parameter α is set to 13. Tables 1 and 2 present the quantitative evaluation of the segmentation results corresponding to different values of parameter α .

Figures 1 and 2 show the segmentation results of the two noisy images. It is observed that the KSSFCM_S algorithm proposed in this study is feasible and can help accurately extract the real target of the noise interference images. Moreover, the two images indicate that the KSSFCM_S algorithm proposed in this study has a certain level of suppressing the noise ability and enhance the antinoise robustness of the semisupervised fuzzy clustering.

Tables 1 and 2 show the quantitative evaluation results. It is observed that the values of α in the range of 10 to 15 are reasonable. Meanwhile, the parameter α varies within the range of [10, 15] and its influence on the segmentation results is not significant. In order to compare the performance differences of different algorithms, the parameter α is selected as 13 in the subsequent tests.

6.2. Performance Comparisons of SSFCM, SSFCM_S, and KSSFCM_S Algorithms. In order to verify that the SSFCM_S and KSSFCM_S algorithms proposed in this paper have reasonable antinoise ability and their segmentation performance of image corrupted by noise is better than the SSFCM algorithm, Figure 3 shows that four gray images are selected for segmentation test. Different mean variances of the Gaussian noise are added to the two synthetic images of subimages (a) and (b). Moreover, different intensities of salt-and-pepper noise are added to the two binary images of subimages (c) and (d). Then, the noise-added images are segmented and tested. For the above-mentioned fuzzy clustering segmentation algorithms, the parameters $\alpha = 13$ and $\tau = 3.8$ are selected and the algorithm is used for the termination conditions $\varepsilon = 0.0001$.

6.2.1. Test and Analysis of the Synthetic Image with Gaussian Noise. A Gaussian noise with mean value of 0 and mean square variances of 57, 80, and 114 are added to the three-valued composite image illustrated in Figure 3(a). It should be indicated that the size of the map is 165×165 and gray values are 0, 105, and 255, respectively. Three different algorithms are tested for whether they can accurately segment different pixel regions and reduce noise points as much as possible or not. Figure 4 shows the detailed segmentation results. Moreover, Table 3 shows the evaluation results of the antinoise robustness and the effectiveness of the segmentation process.

Figure 4 shows that when the Gaussian noise mean variance is 57, three different algorithms can correctly segment the composite images. However, the SSFCM algorithm has a small number of noise points in the segmentation results. When the mean variance of the Gaussian noise increases gradually, the segmentation results of the SSFCM algorithm have obvious misclassification phenomenon; meanwhile the SSFCM_S algorithm and the KSSFCM_S algorithm obtain better segmentation effects. Moreover, the segmentation results of the KSSFCM_S algorithm have relatively few noise points. Therefore, the proposed algorithm has much stronger noise suppression ability.

Table 3 shows that the KSSFCM_S algorithm does not only have the best segmentation performance but also obtains the strongest suppression ability for image with Gaussian noise. However, when the mean square variance of the Gaussian noise increases, the noise suppression ability of the three kinds of robust semisupervised fuzzy clustering algorithms gradually decreases. However, the suppression ability of Gaussian noise with different mean square variances of the proposed KSSFCM_S algorithm does not change, which indicates that the algorithm proposed in this paper obtains strong robustness and adaptability to different intensity of Gaussian noise.

Noisy images corrupted by Gaussian noise with a mean value of 0 and mean square variances of 57, 80, and 114 are added to the four-value images shown in Figure 3(b). It indicates that the size of the image is 246×246 , and its gray values are 32, 78, 156, and 255 for segmentation tests. Since

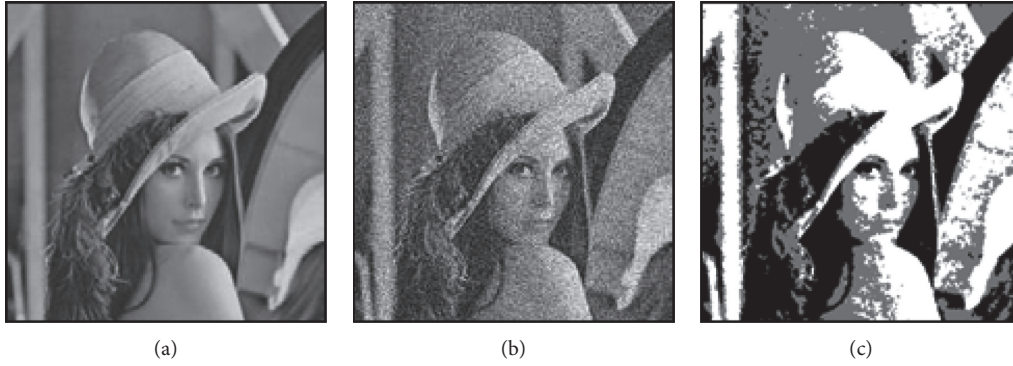


FIGURE 1: Lena image, image with Gaussian noise, and its segmentation result. (a) Original image, (b) noisy image, and (c) segmentation result.

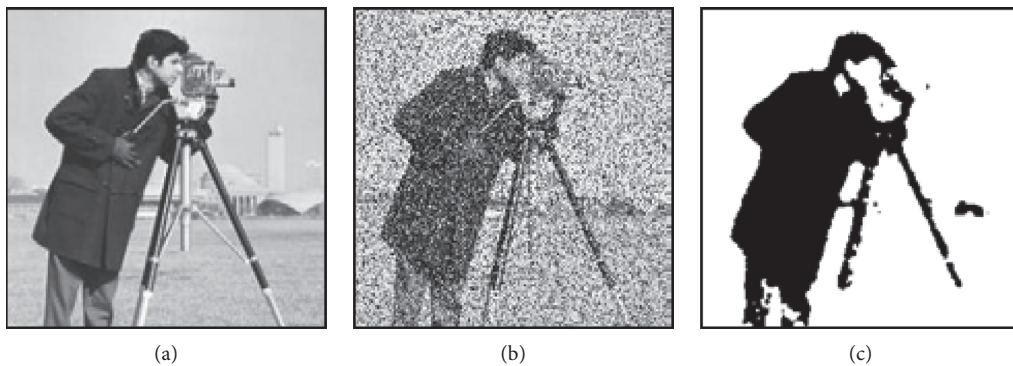


FIGURE 2: Cameraman image, image with salt-and-pepper noise, and its segmentation result. (a) Original image, (b) noisy image, and (c) segmentation result.

TABLE 1: Quantitative evaluation index of segmentation results of noisy Lena image under different α values.

| α | PSNR (dB) | SA (%) |
|----------|-----------|--------|
| 10 | 13.9987 | 84.51 |
| 11 | 14.0280 | 84.67 |
| 12 | 14.0415 | 84.77 |
| 13 | 14.0473 | 84.88 |
| 14 | 14.0556 | 84.97 |
| 15 | 14.0601 | 85.03 |

TABLE 2: Quantitative evaluation index of segmentation results of noisy cameraman images under different α values.

| α | PSNR (dB) | SA (%) |
|----------|-----------|--------|
| 10 | 17.2834 | 98.13 |
| 11 | 17.3513 | 98.16 |
| 12 | 17.3839 | 98.17 |
| 13 | 17.4570 | 98.20 |
| 14 | 17.5127 | 98.23 |
| 15 | 17.5919 | 98.26 |

the number of clusters is 4, it is difficult to effectively segment image corrupted by noise, while it can better explain the robustness and universality of the semisupervised fuzzy segmentation algorithm proposed in this paper. Figure 5

shows the segmentation results obtained by adopting three different robust semisupervised fuzzy clustering segmentation algorithms. Moreover, Table 4 shows the modified peak signal-to-noise ratio and the segmentation accuracy between the practical segmentation results and the ideal segmentation results.

Figure 5 shows that Gaussian noise with different mean square variance is added to the four-value composite image, and the corresponding noise corrupting images cannot correctly extract different subtarget regions of the composite images by using the SSFCM algorithm. Moreover, the noise points in the segmentation result are very obvious. When the mean variance of the Gaussian noise is small, the segmentation results of SSFCM_S and the KSSFCM_S algorithms have only a small number of noise points, which is close to the ideal segmentation images. When the mean variance of the Gaussian noise gradually increases to 114, the SSFCM_S algorithm produces the most serious misclassification phenomenon. However, it can accurately extract 4 different subtarget regions. Moreover, it is indicated that although the segmentation result obtained by the KSSFCM_S algorithm proposed in this paper has only a small number of noise points, it can accurately extract the four subregions of the images and can keep the contour edges clear, which has stronger target acquisition ability than the SSFCM_S algorithm. Therefore, the KSSFCM_S algorithm proposed in this paper has better segmentation ability

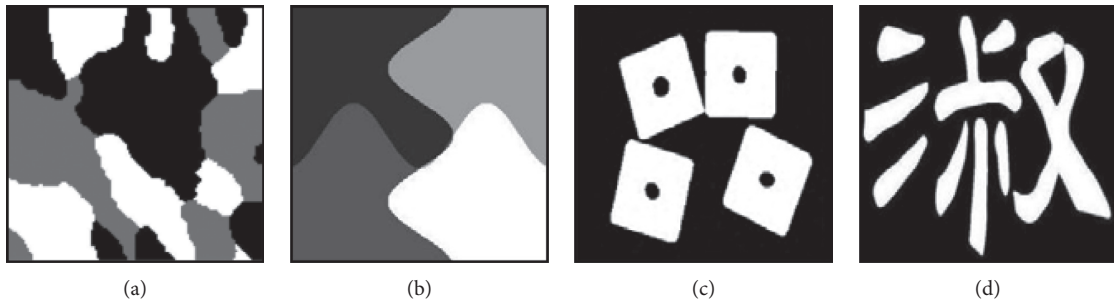


FIGURE 3: Original images. (a) Three-valued synthetic image, (b) four-valued synthetic image, (c) square target image, and (d) Chinese character image.

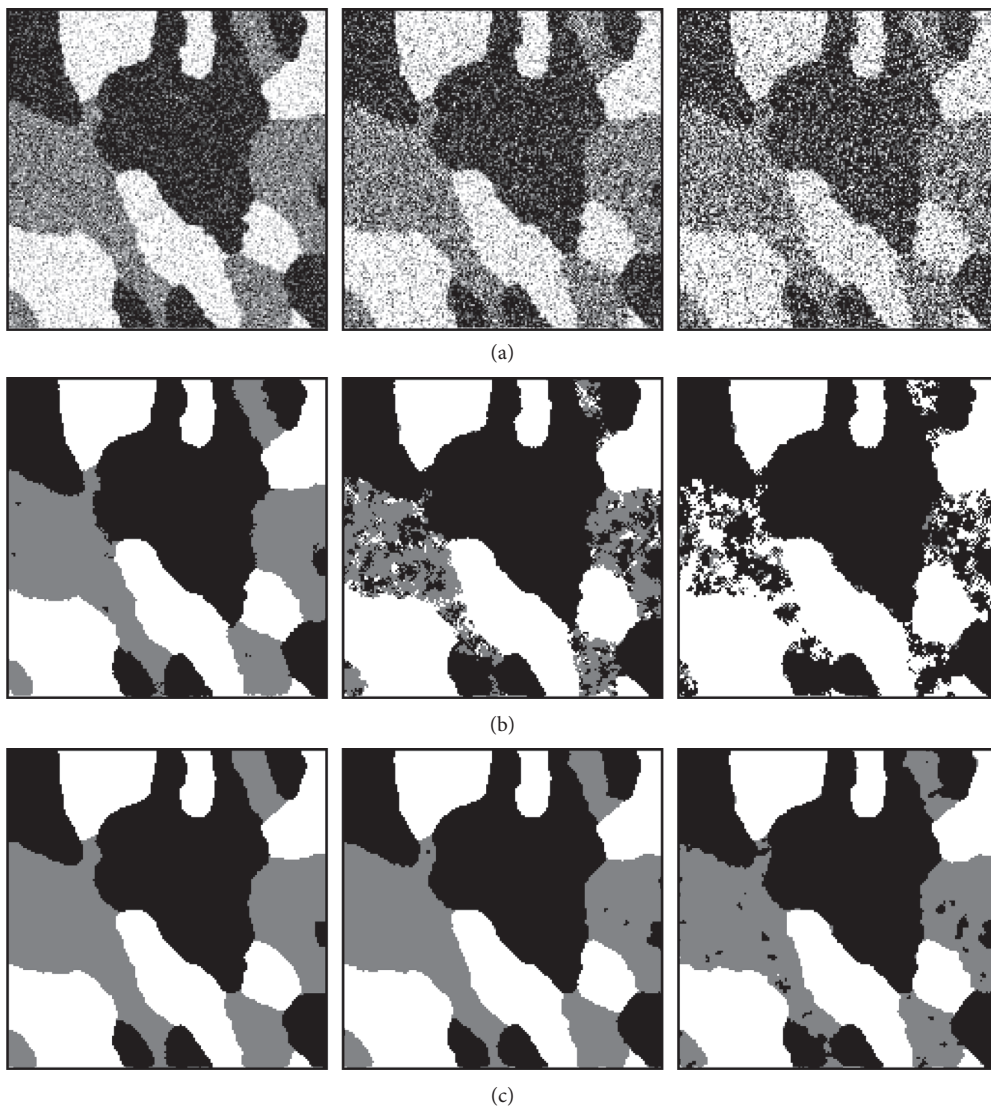


FIGURE 4: Continued.

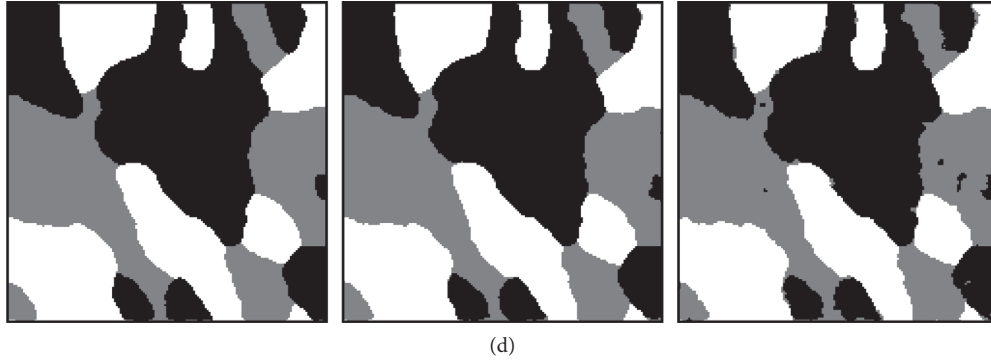


FIGURE 4: Three-valued synthetic image with Gaussian noise and different segmentation results with three classes. (a) Noisy image with mean square variances of 57, 80, and 114 from the left to the right. (b) SSFCM algorithm. (c) SSFCM_S algorithm. (d) KSSFCM_S algorithm.

TABLE 3: PSNR and SA of different algorithms against Gaussian noise.

| Mean variance | Index | SSFCM | SSFCM_S | KSSFCM_S |
|---------------|-----------|---------|---------|----------|
| 57 | PSNR (dB) | 19.6476 | 23.2948 | 23.1314 |
| | SA (%) | 96.62 | 98.71 | 98.73 |
| 80 | PSNR (dB) | 13.8179 | 21.7370 | 22.3103 |
| | SA (%) | 83.67 | 97.88 | 98.34 |
| 114 | PSNR (dB) | 10.9423 | 18.8017 | 20.3733 |
| | SA (%) | 70.66 | 95.24 | 97.01 |

than the other two segmentation algorithms. Furthermore, it can effectively extract the real subtarget contained in the image, thereby showing reasonable clustering performance.

Table 4 shows the quantitative evaluation of the segmentation results for the different four-valued synthetic image corrupted by Gaussian noise. It is observed that the SSFCM_S and the KSSFCM_S algorithms have the same ability of suppressing noise when mean square variance of Gaussian noise is small. However, as mean square variance of Gaussian noise increases, the difference of suppression noise ability between SSFCM_S and KSSFCM_S algorithm is gradually reveal. When mean square variance of Gaussian noise is greater than 100, the segmentation performance and noise suppression capability of KSSFCM_S algorithm are almost twice those of the existing SSFCM algorithm. Moreover, the SSFCM_S algorithm is significantly improved, which makes the KSSFCM_S algorithm more effective than the SSFCM_S algorithm.

6.2.2. Test and Analysis of Binary Image with Salt-and-Pepper Noise. Figure 3(c) shows that the salt-and-pepper noise with intensity of 30%, 50%, and 60% is added to the binary square target image with the size of 241×241 for the segmentation test. Then, the image corrupted by salt-and-pepper noise is segmented by the SSFCM, SSFCM_S, and KSSFCM_S algorithms. Figure 6 shows the segmentation results of the salt-and-pepper corrupting image. Table 5 presents the modified peak signal-to-noise ratio and the correct segmentation rate.

Figure 6 shows the segmentation results obtained from the binary square target image corrupted by salt-and-pepper

noise with different intensities. It is observed that, for the binary-value square target image corrupted by salt-and-pepper noise with low intensity, the segmentation performance of this algorithm is basically not much different. However, as the intensity of salt-and-pepper noise increases, the segmentation results of the three different algorithms have some differences, but they are not significant. Moreover, if the intensity of salt-and-pepper noise exceeds 50%, the weak performance of the SSFCM algorithm is revealed. Furthermore, the edge of the target in segmentation results becomes very jagged, resulting in an uneven edge. On the other hand, for square target image corrupted by salt-and-pepper noise with high intensity, the segmentation results of the SSFCM_S and the KSSFCM_S algorithms do not show significant differences; meanwhile the edge contour of the extracted target in segmentation results is clear and smooth.

Table 5 shows the quantitative evaluation of segmentation results of the binary-valued square target image corrupted by salt-and-pepper noise with different intensities. It is observed that if salt-and-pepper noise with low intensity is added to the square target image, the segmentation performance and antinoise ability of three different segmentation algorithms are basically equivalent. However, if the intensity of salt-and-pepper noise increases, the difference of antinoise ability between the SSFCM_S, the KSSFCM_S, and the SSFCM algorithms gradually appears. It is indicated that if the intensity of salt-and-pepper exceeds 50%, the segmentation performance and antinoise ability of the SSFCM algorithm decrease significantly. Moreover, the segmentation performance and antinoise ability of the SSFCM_S algorithm and the KSSFCM_S algorithm also decrease to some extent; however the reduction degree is not obvious. Especially when the intensity of salt-and-pepper noise is high, the SSFCM_S algorithm and the KSSFCM_S algorithm show the same segmentation performance and antinoise ability for this simple binary-valued square target image.

Figure 3(d) shows that salt-and-pepper noise with intensity of 30%, 40%, and 50% is added to the “Shu” in the Chinese character image with the size of 256×256 . Then, the image corrupted by noise is segmented by using the SSFCM algorithm. Figure 7 shows the segmentation results obtained by the SSFCM_S and the KSSFCM_S algorithms. Moreover, Table 6 presents the results of the quantitative evaluation of

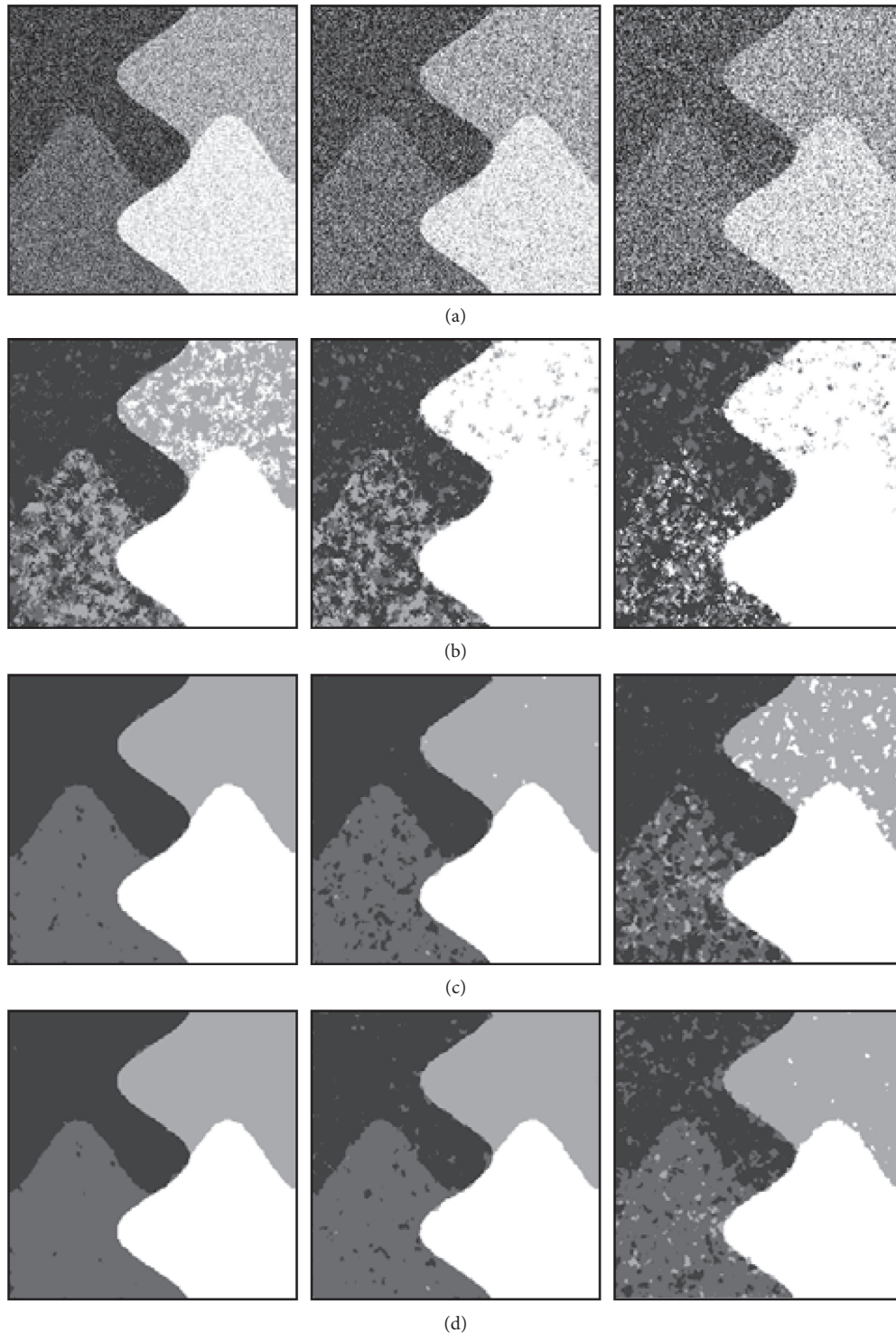


FIGURE 5: Synthetic images with Gaussian noise and different segmentation results with four classes. (a) Image corrupted by Gaussian noise with mean square variances of 57, 80, and 114 from left to right. (b) SSFCM algorithm. (c) SSFCM_S algorithm. (d) KSSFCM_S algorithm.

the segmentation results by using the modified peak signal-to-noise ratio and segmentation accuracy.

Figure 7 shows the segmentation results of the “Shu” Chinese character image corrupted by salt-and-pepper with different intensities. It is indicated that if the intensity of salt-and-pepper noise is low, the segmentation results obtained

by three segmentation algorithms are the same, and the extracted Chinese characters from noisy image are smoother. However, if the intensity of salt-and-pepper noise is 50%, the segmentation result has a few of noise points; meanwhile, its target edge is not smooth. It shows that the segmentation performance of the SSFCM algorithm has a

TABLE 4: The PSNR and SA of different algorithms against Gaussian noise.

| Mean variance | Index | SSFCM | SSFCM_S | KSSFCM_S |
|---------------|-----------|---------|---------|----------|
| 57 | PSNR (dB) | 16.2111 | 29.6277 | 30.2835 |
| | SA (%) | 73.53 | 98.85 | 99.25 |
| 80 | PSNR (dB) | 12.9310 | 25.9271 | 27.9348 |
| | SA (%) | 54.45 | 95.80 | 97.79 |
| 114 | PSNR (dB) | 12.0983 | 19.6946 | 23.2612 |
| | SA (%) | 52.06 | 84.94 | 91.63 |

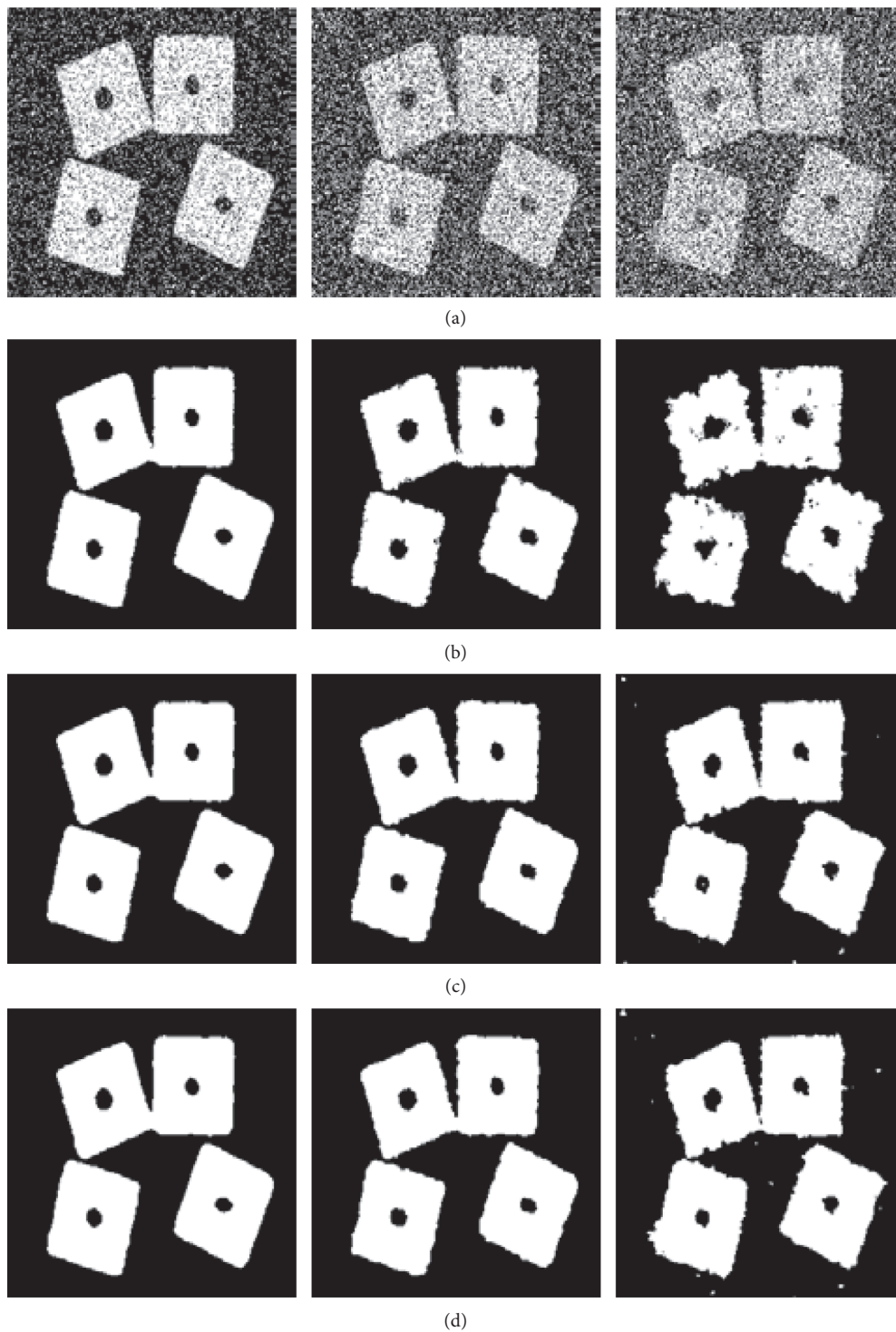


FIGURE 6: Noisy square target images and different segmentation results. (a) Image corrupted by salt-and-pepper with intensity of 30%, 50%, and 60% from left to right. (b) SSFCM algorithm. (c) SSFCM_S algorithm. (d) KSSFCM_S algorithm.

TABLE 5: The PSNR and SA of different algorithms against salt-and-pepper noise.

| Intensity | Index | SSFCM | SSFCM_S | KSSFCM_S |
|-----------|-----------|---------|---------|----------|
| 30 | PSNR (dB) | 22.6161 | 22.0894 | 22.0293 |
| | SA (%) | 99.45 | 99.38 | 99.37 |
| 50 | PSNR (dB) | 18.2501 | 19.5246 | 19.7234 |
| | SA (%) | 98.50 | 98.88 | 98.93 |
| 60 | PSNR (dB) | 13.9538 | 17.4533 | 17.2621 |
| | SA (%) | 95.98 | 98.20 | 98.12 |

sharp decline for the image with high salt-and-pepper noise. Furthermore, the SSFCM_S and KSSFCM_S algorithms can accurately extract Chinese character targets. Moreover, the contours of Chinese characters are neat and very smooth, which shows that KSSFCM_S algorithm has significant and potential advantages compared with the SSFCM algorithm for segmentation image with high salt-and-pepper noise.

Table 6 shows the quantitative evaluation of the segmentation results. It is indicated that if the intensity of salt-and-pepper noise is low, the SSFCM_S and the KSSFCM_S algorithms have no obvious advantages compared with the SSFCM algorithm. As the intensity of salt- and-pepper noise increases, the advantages of the SSFCM_S and the KSSFCM_S algorithms compared with the SSFCM algorithm gradually appear. When the intensity of the salt-and-pepper noise reaches 50%, the weak antinoise ability of the SSFCM algorithm is revealed. Moreover, the target edge of the Chinese character extracted by the SSFCM algorithm is obviously blurred, and its edge smoothness degree is far worse than the normal Chinese character. However, the SSFCM_S and the KSSFCM_S algorithms show reasonable segmentation robustness to the image corrupted by salt-and-pepper with high intensity. Moreover, their segmentation results are basically equivalent to the segmentation results of the image corrupted by salt-and-pepper with low intensity. Furthermore, the changes in the PSNR and SA are not obvious, which indicates that the SSFCM_S and the KSSFCM_S algorithms have good adaptability to salt-and-pepper noise with different intensity.

6.3. Analyzing KSSFCM_S and Existing Fuzzy Algorithms.

In this section, the segmentation results of the proposed KSSFCM_S algorithm are compared with those of other robust clustering algorithms. In this regard, four typical algorithms, including the FCM_S [2], FLICM [20], KWFLICM [22], and the LMDKLICM [55] are considered for analyzing the clustering performance and noise suppression ability of different algorithms. Moreover, it is intended to evaluate performance of the proposed KSSFCM_S algorithm. Two medical images and two remote sensing images are shown in Figure 8. In order to provide degraded medical images, different Gaussian noises with mean 0 and mean square variances of 80 and 114 are added to the medical image 1 with size of 423×478 and the medical image 2 with size of 256×256 , respectively.

Moreover, the salt-and-pepper noise with 30% intensity is added into the remote sensing image 1 with the size of 245×176 and the remote sensing image 2 with the size of

352×300 . The above-mentioned five fuzzy clustering segmentation algorithms are applied to segment noisy images. Figures 9 and 10 show the obtained segmentation results. Furthermore, Tables 7 and 8 show the modified peak signal-to-noise ratio (SNR) values and segmentation correctness rates of different segmentation algorithms.

Figure 9 indicates that the segmentation results obtained from the SSFCM algorithm have obvious noise points, which shows the weak performance of the SSFCM algorithm to suppress Gaussian noise. In other words, it is found that the SSFCM algorithm cannot obtain satisfactory segmentation effects. The noise points of segmentation results not only affect the effective identification of medical targets but also seriously interfere with the clinical medical diagnosis. However, the application of the FLICM, KWFLICM, and the LMDKFCM algorithms can effectively suppress Gaussian noise in segmented image so that the noise points significantly reduce in the segmentation results and the edge of extracted target becomes clear. More specifically, almost no noise points remain in the segmentation results obtained from the KWFLICM algorithm. Moreover, it is found that there is no noise in the segmentation results obtained from the proposed KSSFCM_S algorithm. Meanwhile, the main shortcoming of these methods is difficult to retain the detail feature of noisy image. In comparison, the proposed KSSFCM_S algorithm can obtain satisfactory segmentation results for medical image 1 corrupted by high Gaussian noise; meanwhile the segmentation results of medical image 2 with Gaussian noise are slightly insufficient, which may be due to the loss of some details.

Table 7 shows the quantitative evaluation of the segmentation results of two medical images corrupted by Gaussian noise. It indicates that the segmentation performance of the KSSFCM_S algorithm is significantly better than that of the FCM_S algorithm. In fact, it is observed that the suppressing noise ability of KSSFCM_S is almost twice as good as that of FCM_S algorithm. However, the segmentation performance of the KSSFCM_S algorithm in comparison with the FLICM, KWFLICM, and the LMDKLFCM algorithms is slightly improved to a certain extent. This makes the proposed KSSFCM_S algorithm have a certain degree of advantage for segmenting image with high Gaussian noise.

Figure 10 illustrates the segmentation results of two remote sensing images corrupted by salt-and-pepper noise. It is observed that the FCM_S algorithm cannot effectively extract the remote sensing target from noisy image, resulting in obvious noise points in the segmentation results, which are not conducive for recognizing and understanding the

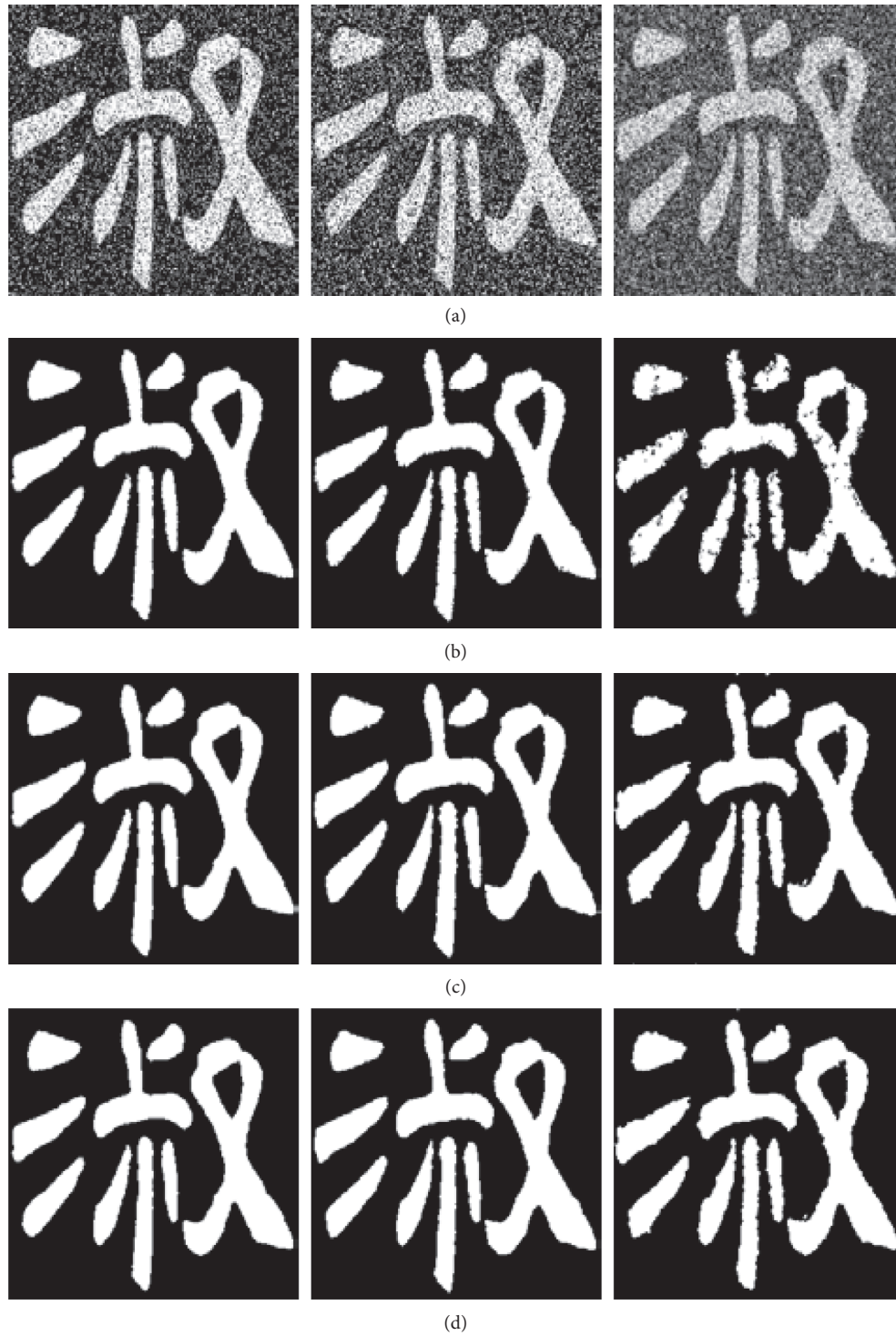


FIGURE 7: Chinese character images with salt-and-pepper noise and different segmentation results. (a) Image corrupted by salt-and-pepper noise with intensity of 30%, 40%, and 50% from left to right. (b) SSFCM algorithm. (c) SSFCM_S algorithm. (d) KSSFCM_S algorithm.

TABLE 6: The PSNR and SA of different algorithms against salt-and-pepper noise.

| Intensity (%) | Index | SSFCM | SSFCM_S | KSSFCM_S |
|---------------|-----------|---------|---------|----------|
| 30 | PSNR (dB) | 20.0827 | 20.0894 | 19.9366 |
| | SA (%) | 99.02 | 99.02 | 98.99 |
| 40 | PSNR (dB) | 18.2084 | 19.0586 | 19.1448 |
| | SA (%) | 98.49 | 98.76 | 98.78 |
| 50 | PSNR (dB) | 13.3246 | 17.3948 | 17.7667 |
| | SA (%) | 95.35 | 98.18 | 98.33 |

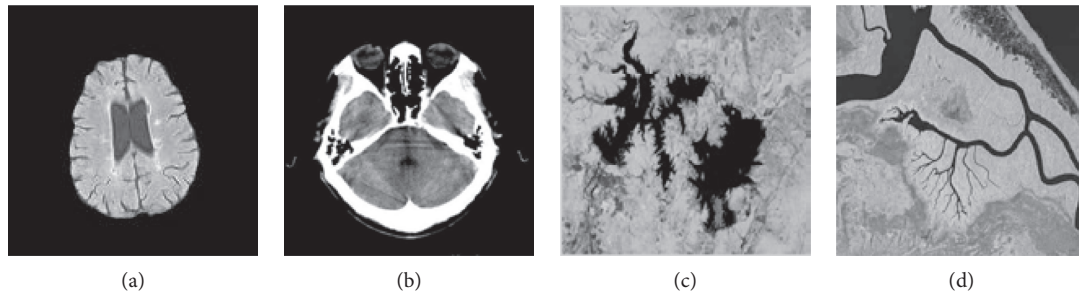


FIGURE 8: Original images. (a) Medical image 1, (b) medical image 2, (c) remote sensing image 1, and (d) remote sensing image 2.

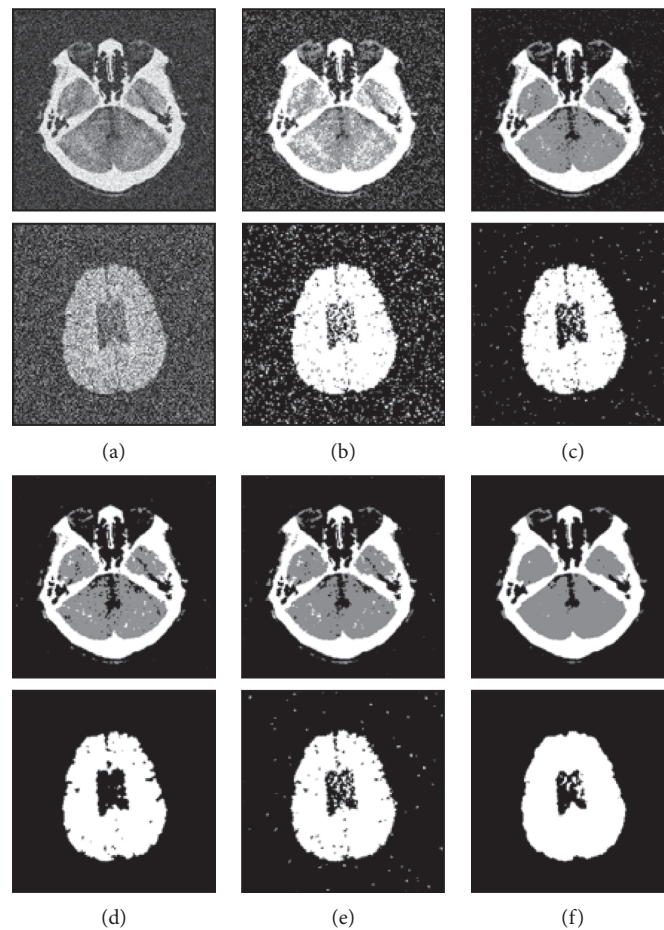


FIGURE 9: Different segmentation results of medical images with Gaussian noise. (a) Noisy image, (b) FCM_S, (c) FLICM, (d) KWFLICM, (e) LMDKLCM, and (f) KSSFCM_S.

target. However, it is found that application of the FLICM and the LMDKLCM algorithms can effectively suppress the noise points of remote sensing images corrupted by salt-and-pepper noise so that noise pixels in the segmentation results significantly reduce. Moreover, almost no noise remains in the segmentation results obtained from the KWFLICM and the KSSFCM_S algorithms so that remote sensing targets in the noisy image are accurately extracted. It is concluded that the target extracted by the proposed KSSFCM_S algorithm is more accurate than that of the KWFLICM algorithm, while

the KWFLICM algorithm slightly misinterprets the background or the noise into targets.

Table 8 shows the quantitative evaluation of the segmentation results obtained from remote sensing images corrupted by high salt-and-pepper noise. It is observed that the clustering performance of the KSSFCM_S algorithm is much better than that of the FCM_S algorithm. More specifically, the suppression ability of salt-and-pepper noise is almost three times that for the FCM_S algorithm. Table 8 indicates that the proposed KSSFCM_S algorithm has

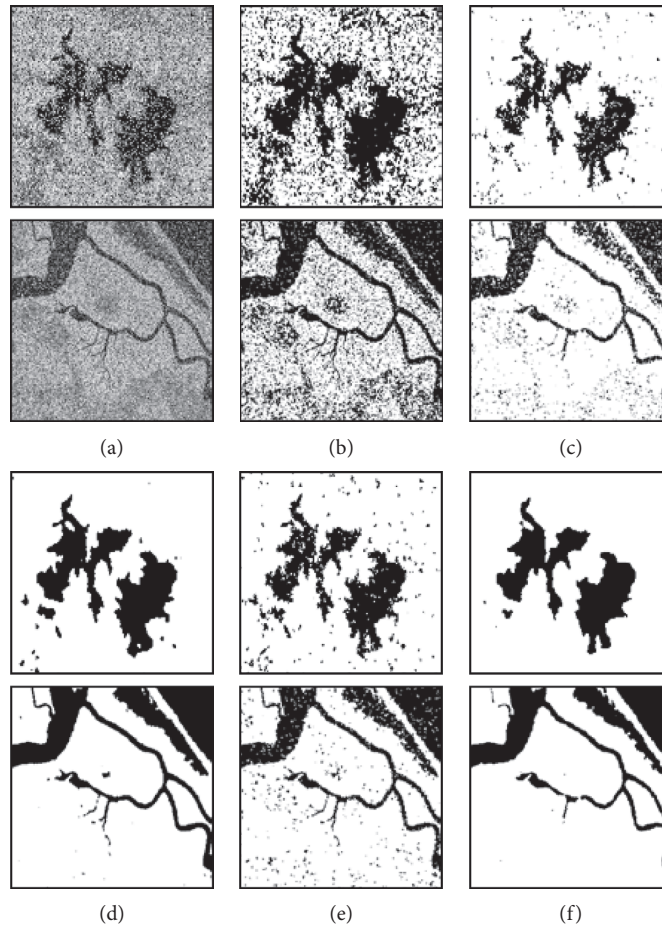


FIGURE 10: Remote sensing images with salt-and-pepper noise and segmentation results by different robust fuzzy clustering algorithms. (a) Noisy image, (b) FCM_S, (c) FLICM, (d) KWFLICM, (e) LMDKLFM, and (f) KSSFCM_S.

TABLE 7: PSNR and SA of different algorithms against Gaussian noise.

| | Index | FCM_S | FLICM | KWFLICM | LMDKLFM | KSSFCM_S |
|-----------------|-----------|---------|---------|---------|---------|----------|
| Medical image 1 | PSNR (dB) | 12.5220 | 19.1125 | 19.9467 | 20.5600 | 22.4596 |
| | SA (%) | 77.34 | 95.01 | 96.01 | 96.63 | 98.16 |
| Medical image 2 | PSNR (dB) | 10.7426 | 15.8382 | 18.1478 | 16.5521 | 19.2548 |
| | SA (%) | 91.57 | 97.39 | 98.47 | 97.79 | 98.81 |

TABLE 8: PSNR and SA of different algorithms against salt-and-pepper noise.

| | Index | FCM_S | FLICM | KWFLICM | LMDKLFM | KSSFCM_S |
|------------------------|-----------|--------|---------|---------|---------|----------|
| Remote sensing image 1 | PSNR (dB) | 6.4576 | 12.6900 | 17.0373 | 13.3148 | 18.2714 |
| | SA (%) | 77.39 | 94.62 | 98.02 | 95.34 | 98.51 |
| Remote sensing image 2 | PSNR (dB) | 6.6449 | 11.2401 | 19.4848 | 13.3507 | 18.1015 |
| | SA (%) | 78.35 | 92.48 | 98.87 | 95.38 | 98.45 |

slightly better clustering performance in comparison with the FLICM and LMDKLFM algorithms. This superiority is especially more pronounced for the suppression of salt-and-pepper noise. It is concluded that the proposed algorithm is almost 0.5 times higher than the two typical robust clustering algorithms. However, compared with the KWFLICM

algorithm, the proposed KSSFCM_S algorithm has the same level of the clustering performance and antinoise ability.

Figure 10 shows the remote sensing image 2 corrupted by high salt-and-pepper noise. It should be indicated that this image is applied in testing the time cost of different algorithms, including the FCM_S, FLICM, KWFLICM,

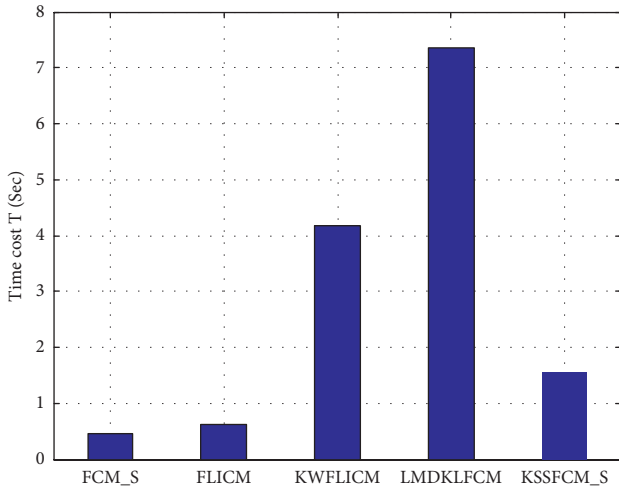


FIGURE 11: Time cost of different algorithms for remote sensing image 2.

LMDKLFM, and the KSSFCM_S algorithms. Figure 11 illustrates the time cost of different algorithms. It is observed that the FCM_S algorithm takes the least time, followed by the FLICM algorithm. Moreover, it is found that the LMDKLFM algorithm takes the longest time. Therefore, it is concluded that the LMDKLFM algorithm is an inappropriate scheme for applications with high real-time requirements, including target tracking, intelligent traffic, industrial automation, and robot vision. Comparison of the running time between the KWFLICM algorithm and the proposed KSSFCM_S algorithm shows obvious superiorities of the proposed algorithm.

Considering the foregoing tests and analysis on different algorithms, it is concluded that the proposed KSSFCM_S algorithm has certain potential advantages in numerous applications compared with the FLICM and the KWFLICM algorithms. The development of robust fuzzy clustering algorithms can effectively solve the segmentation problems of images corrupted by high noise and can have certain values for image understanding and machine vision applications.

6.4. Deep Analysis of the Proposed and Other Algorithms. The fuzzy clustering algorithm with partial supervision proposed by Pedrycz [30] used labelled patterns to enhance sample clustering performance; thus it is incorporating the prior membership information of clustering sample into the objective function of fuzzy clustering, and a semisupervision fuzzy clustering is obtained to solve the problem of existing fuzzy clustering.

In our proposed method, we replaced the partial labelled information with mean value of membership from the neighborhood window around the central pixel. The reason why we do that is because the neighborhood pixel can play an important role in the classification membership degree of the central pixel based on high correlation between central pixel and its neighborhood pixels. Meanwhile, we set the values of Boolean vector all equal to “1” because we need the

membership information of neighborhood pixels. Besides, we incorporate the spatial information constraints which calculate the gray difference between mean value of neighborhood pixels and class centers into the proposed objective function to improve the antinoise performance. Furthermore, as for the parameter used as a regular term control factor, we determine the value of the regularized factor from literature [3].

As a result, compared with Pedrycz’s algorithm, we fully consider the characteristics difference of digital images and structured data and propose more reasonable supervised information which come from the mean membership of neighborhood pixels. And compared with other robust fuzzy clustering algorithms like FCM_S, FLICM, and KWFLICM, the idea of our proposed method has obvious novelty. Our proposed method is based on the semisupervised fuzzy clustering with multiple spatial information constraints, but other fuzzy clustering algorithms are unsupervised fuzzy clustering with spatial information constraints.

In addition, the proposed robust semisupervised fuzzy clustering with multiple information constraints is inspired by the process from literature [19] to literature [20], so that the proposed algorithm has good segmentation performance and antinoise ability.

7. Conclusions

Based on the existing semisupervised fuzzy clustering theories, the present study expands and promotes the conventional SSFCM algorithm. Since the SSFCM algorithm is sensitive to noise, the construction idea of the FCM_S1 scheme is utilized to propose an improved robust SSFCM_S segmentation algorithm. Besides, Gaussian kernel function is introduced to enhance the segmentation performance of the robust SSFCM_S algorithm. In this regard, a robust KSSFCM_S segmentation algorithm with certain universality is obtained. Experiment results indicate that the introduction of local neighborhood information can improve the antinoise robustness of semisupervised algorithms for image segmentation. It is concluded that the KSSFCM_S algorithm yields more satisfactory results than the SSFCM_S algorithm does. Moreover, it is found that the proposed algorithm can meet the requirements of segmentation image with strong noise in various real-time applications.

The present study shows that to enhance the robustness of the constrained fuzzy clustering for the image segmentation, the idea of the robust semisupervised fuzzy clustering can be extended to the constrained semisupervised fuzzy clustering. It is concluded that the robust semisupervised fuzzy clustering promotes the semisupervised fuzzy clustering to solve the effective interpretation of the complex medical and remote sensing images.

Data Availability

The image data used to support the findings of this study are included within the supplementary information file. And the image data used to support the findings of this study are available from the corresponding author upon request.

Conflicts of Interest

The authors declare that they have no conflicts of interest.

References

- [1] J. Nayak, B. Naik, and H. S. Behera, "Fuzzy C-means (FCM) clustering algorithm: a decade review from 2000 to 2014," *Computational Intelligence in Data Mining-Volume 2*, pp. 133–149, Springer, Berlin, Germany, 2015.
- [2] M. N. Ahmed, S. M. Yamany, N. Mohamed, A. A. Farag, and T. Moriarty, "A modified fuzzy C-means algorithm for bias field estimation and segmentation of MRI data," *IEEE Transactions on Medical Imaging*, vol. 21, no. 3, pp. 193–199, 2002.
- [3] S. C. Chen and D. Q. Zhang, "Robust image segmentation using FCM with spatial constraints based on new kernel-induced distance measure," *IEEE Transactions on Systems, Man, and Cybernetics-Part B: Cybernetics*, vol. 34, no. 4, pp. 190–1916, 2004.
- [4] F. Zhao, L. C. Jiao, H. Q. Liu, and X. Gao, "A novel fuzzy clustering algorithm with non local adaptive spatial constraint for image segmentation," *Signal Processing*, vol. 91, no. 4, pp. 988–999, 2011.
- [5] F. Zhao, H. Q. Liu, and J. L. Fan, "Multi-objective evolutionary clustering with complementary spatial information for image segmentation," *Journal of Electronics & Information Technology*, vol. 37, no. 3, pp. 672–678, 2015.
- [6] L. Guo, L. Chen, C. L. Philip, and J. Zhou, "Integrating guided filter into fuzzy clustering for noisy image segmentation," *Digital Signal Processing*, vol. 83, pp. 235–248, 2018.
- [7] J. Gu, L. Jiao, S. Yang, and J. Zhou, "Sparse learning based fuzzy c-means clustering," *Knowledge-Based Systems*, vol. 119, pp. 113–125, 2017.
- [8] M.-S. Yang and H.-S. Tsai, "A Gaussian kernel-based fuzzy C-means algorithm with a spatial bias correction," *Pattern Recognition Letters*, vol. 29, no. 12, pp. 1713–1725, 2008.
- [9] J. Wang, J. Kong, Y. Lu, M. Qi, and B. Zhang, "A modified FCM algorithm for MRI brain image segmentation using both local and non-local spatial constraints," *Computerized Medical Imaging and Graphics*, vol. 32, no. 8, pp. 685–698, 2008.
- [10] S. Belhassen and H. Zaidi, "A novel fuzzy C-means algorithm for unsupervised heterogeneous tumor quantification in PET," *Medical Physics*, vol. 37, no. 3, pp. 1309–1324, 2010.
- [11] Z. Wang, Q. Song, Y. C. Soh, and K. Sim, "An adaptive spatial information-theoretic fuzzy clustering algorithm for image segmentation," *Computer Vision and Image Understanding*, vol. 117, no. 10, pp. 1412–1420, 2013.
- [12] Y. K. Dubey and M. M. Mushrif, "FCM clustering algorithms for segmentation of brain MR images," *Advances in Fuzzy Systems*, vol. 2016, Article ID 3406406, 14 pages, 2016.
- [13] Y. F. Zhong, A. L. Ma, and L. P. Zhang, "An adaptive memetic fuzzy clustering algorithm with spatial information for remote sensing imagery," *IEEE Journal of Selected Topics in Applied Earth Observation and Remote Sensing*, vol. 7, no. 4, pp. 1235–1248, 2014.
- [14] K.-S. Chuang, H.-L. Tzeng, S. Chen, J. Wu, and T.-J. Chen, "Fuzzy C-means clustering with spatial information for image segmentation," *Computerized Medical Imaging and Graphics*, vol. 30, no. 1, pp. 9–15, 2006.
- [15] S. K. Adhikari, J. K. Sing, D. K. Basu, and M. Nasipuri, "Conditional spatial fuzzy C-means clustering algorithm for segmentation of MRI images," *Applied Soft Computing*, vol. 34, pp. 758–769, 2015.
- [16] W. Cai, S. Chen, and D. Zhang, "Fast and robust fuzzy C-means clustering algorithms incorporating local information for image segmentation," *Pattern Recognition*, vol. 40, no. 3, pp. 825–838, 2007.
- [17] D. L. Pham, "Spatial models for fuzzy clustering," *Computer Vision and Image Understanding*, vol. 84, no. 2, pp. 285–297, 2001.
- [18] D.-Q. Zhang and S.-C. Chen, "A novel kernelized fuzzy C-means algorithm with application in medical image segmentation," *Artificial Intelligence in Medicine*, vol. 32, no. 1, pp. 37–50, 2004.
- [19] Y. Yang and S. Y. Huang, "Image segmentation by fuzzy C-means clustering algorithm with a novel penalty term," *Computing and Informatics*, vol. 26, no. 1, pp. 17–31, 2007.
- [20] S. Krinidis and V. Chatzis, "A robust fuzzy local information C-means clustering algorithm," *IEEE Transactions on Image Processing*, vol. 19, no. 5, pp. 1328–1337, 2010.
- [21] N. Li, H. Huo, Y.-M. Zhao, X. Chen, and T. Fang, "A spatial clustering method with edge weighting for image segmentation," *IEEE Geoscience and Remote Sensing Letters*, vol. 10, no. 5, pp. 1124–1128, 2013.
- [22] M. Gong, Y. Liang, J. Shi, W. Ma, and J. Ma, "Fuzzy C-means clustering with local information and kernel metric for image segmentation," *IEEE Transactions on Image Processing*, vol. 22, no. 2, pp. 573–584, 2013.
- [23] D. L. Xiang, T. Tang, C. B. Hu, Y. Li, and Y. Su, "A kernel clustering algorithm with fuzzy factor application to SAR image segmentation," *IEEE Geoscience and Remote Sensing Letters*, vol. 11, no. 7, pp. 1290–1294, 2014.
- [24] S. Bhagyalakshmi and V. U. Biju, "Image segmentation using kernel metric and modified weighted fuzzy factor," *International Journal of Engineering Research & Technology (IJERT)*, vol. 4, no. 5, pp. 68–72, 2015.
- [25] K. L. Hemalatha, D. S. Manvi, and D. H. Suresh, "Adaptive weighted covariance regularized kernel fuzzy c means algorithm for medical image segmentation," *Journal of Theoretical and Applied Information Technology*, vol. 95, no. 14, pp. 3365–3375, 2017.
- [26] H. Zhang, L. Bruzzone, W. Shi, M. Hao, and Y. Wang, "Enhanced spatially constrained remotely sensed imagery classification using a fuzzy local double neighborhood information C-means clustering algorithm," *IEEE Journal of Selected Topics in Applied Earth Observations and Remote Sensing*, vol. 11, no. 8, pp. 2896–2910, 2018.
- [27] X. Zhang, Q. Guo, Y. Sun et al., "Patch-based fuzzy clustering for image segmentation," *Soft Computing*, vol. 23, no. 9, pp. 3081–3093, 2019.
- [28] K. Li, Z. Cao, L. Cao et al., "Some developments on semi-supervised clustering," *Pattern Recognition and Artificial Intelligence*, vol. 22, no. 5, pp. 735–742, 2009.
- [29] S. Zeng, X. Tong, N. Sang, and R. Huang, "A study on semi-supervised FCM algorithm," *Knowledge and Information Systems*, vol. 35, no. 3, pp. 585–612, 2013.
- [30] W. Pedrycz, "Algorithms of fuzzy clustering with partial supervision," *Pattern Recognition Letters*, vol. 3, no. 1, pp. 13–20, 1985.
- [31] A. Bouchachia and W. Pedrycz, "Enhancement of fuzzy clustering by mechanisms of partial supervision," *Fuzzy Sets and Systems*, vol. 157, no. 13, pp. 1759–1773, 2006.
- [32] N. Grira, M. Crucianu, and N. Boujemaa, "Active semi-supervised fuzzy clustering," *Pattern Recognition*, vol. 41, no. 5, pp. 1834–1844, 2008.
- [33] J. X. Cai, F. Yang, and G. C. Feng, "Degeneracy-improved semi-supervised fuzzy clustering with application in MR

- image segmentation,” *Journal of Image and Graphics*, vol. 16, no. 5, pp. 784–791, 2011.
- [34] H. Gan, N. Sang, R. Huang, X. Tong, and Z. Dan, “Using clustering analysis to improve semi-supervised classification,” *Neurocomputing*, vol. 101, pp. 290–298, 2013.
- [35] A. A. Abin and H. Beigy, “Active constrained fuzzy clustering: a multiple kernels learning approach,” *Pattern Recognition*, vol. 48, no. 3, pp. 953–967, 2015.
- [36] A. M. Bensaid, L. O. Hall, J. C. Bezdek, and L. P. Clarke, “Partially supervised clustering for image segmentation,” *Pattern Recognition*, vol. 29, no. 5, pp. 859–871, 1996.
- [37] A. Bouchachia and W. Pedrycz, “A semi-supervised clustering algorithm for data exploration,” in *Proceedings of the 10th international fuzzy systems association world congress on fuzzy sets and systems*, pp. 328–337, Istanbul, Turkey, 2003.
- [38] I. A. Maraziotis, “A semi-supervised fuzzy clustering algorithm applied to gene expression data,” *Pattern Recognition*, vol. 45, no. 1, pp. 37–648, 2012.
- [39] M. Fatehi and H. H. Asadi, “Application of semi-supervised fuzzy c-means method in clustering multivariate geochemical data, a case study from the Dalli Cu-Au porphyry deposit in central Iran,” *Ore Geology Reviews*, vol. 81, pp. 245–255, 2017.
- [40] G. Castellano, A. M. Fanelli, and M. A. Torsello, “Shape annotation by semi-supervised fuzzy clustering,” *Information Sciences*, vol. 289, pp. 148–161, 2014.
- [41] C. Zhu, S. Yang, Q. Zhao, S. Cui, and N. Wen, “Robust semi-supervised kernel-FCM algorithm incorporating local spatial information for remote sensing image classification,” *Journal of the Indian Society of Remote Sensing*, vol. 42, no. 1, pp. 35–49, 2014.
- [42] S. D. Mai and L. T. Ngo, “Multiple kernel approach to semi-supervised fuzzy clustering algorithm for land-cover classification,” *Engineering Applications of Artificial Intelligence*, vol. 68, pp. 205–213, 2018.
- [43] P. Shao, W. Shi, P. He, M. Hao, and X. Zhang, “Novel approach to unsupervised change detection based on a robust semi-supervised FCM clustering algorithm,” *Remote Sensing*, vol. 8, no. 3, pp. 264–288, 2016.
- [44] W. Pedrycz and J. Waletzky, “Fuzzy clustering with partial supervision,” *IEEE Transactions on Systems, Man and Cybernetics, Part B (Cybernetics)*, vol. 27, no. 5, pp. 787–795, 1997.
- [45] C. Stutz and T. A. Runkler, “Classification and prediction of road traffic using application-specific fuzzy clustering,” *IEEE Transactions on Fuzzy Systems*, vol. 10, no. 3, pp. 297–308, 2002.
- [46] A. Bouchachia and W. Pedrycz, “Data clustering with partial supervision,” *Data Mining and Knowledge Discovery*, vol. 12, no. 1, pp. 47–78, 2006.
- [47] T. M. Tuan, L. H. Son, and L. B. Dung, “Dynamic semi-supervised fuzzy clustering for dental X-ray image segmentation: an analysis on the additional function,” *Journal of Computer Science and Cybernetics*, vol. 31, no. 4, pp. 323–339, 2015.
- [48] L. H. Son and T. M. Tuan, “A cooperative semi-supervised fuzzy clustering framework for dental X-ray image segmentation,” *Expert Systems with Applications*, vol. 46, pp. 380–393, 2016.
- [49] T. M. Tuan, T. T. Ngan, and L. H. Son, “A novel semi-supervised fuzzy clustering method based on interactive fuzzy satisficing for dental x-ray image segmentation,” *Applied Intelligence*, vol. 45, no. 2, pp. 402–428, 2016.
- [50] L. H. Son and T. M. Tuan, “Dental segmentation from X-ray images using semi-supervised fuzzy clustering with spatial constraints,” *Engineering Applications of Artificial Intelligence*, vol. 59, pp. 186–195, 2017.
- [51] X. Bai, Z. Chen, Y. Zhang, Z. Liu, and Y. Lu, “Infrared ship target segmentation based on spatial information improved FCM,” *IEEE Transactions on Cybernetics*, vol. 46, no. 12, pp. 3259–3271, 2016.
- [52] S. P. Chatzis and T. A. Varvarigou, “A fuzzy clustering approach toward hidden Markov random field models for enhanced spatially constrained image segmentation,” *IEEE Transactions on Fuzzy Systems*, vol. 16, no. 5, pp. 1351–1361, 2008.
- [53] T. M. Nguyen and Q. M. J. Wu, “Dynamic fuzzy clustering and its application in motion segmentation,” *IEEE Transactions on Fuzzy Systems*, vol. 21, no. 6, pp. 1019–1031, 2013.
- [54] G. Liu, Y. Zhang, and A. M. Wang, “Incorporating adaptive local information into fuzzy clustering for image segmentation,” *IEEE Transactions on Image Processing*, vol. 24, no. 11, pp. 3990–4000, 2015.
- [55] R. R. Gharieb, G. Gendy, A. Abdelfattah, and H. Selim, “Adaptive local data and membership based KL divergence incorporating C-means algorithm for fuzzy image segmentation,” *Applied Soft Computing*, vol. 59, pp. 143–152, 2017.
- [56] Q. H. Zhao, S. H. Jia, J. Gao et al., “Fuzzy clustering with spatial constrained membership for image segmentation,” *Science of Surveying and Mapping*, vol. 44, no. 5, pp. 164–170, 2019.
- [57] H. He, X. Yu, and D. Hu, *Fuzzy Uncertainty Analysis Modeling and Application*, Science Press, Beijing, China, 2016.
- [58] W. Zangwill, *Nonlinear Programming: A Unified Approach*, Prentice-Hall, Englewood Cliffs, NJ, USA, 1969.
- [59] F. H. Qu, Y. T. Hu, S. L. Ma et al., “A convergence theorem of kernel based fuzzy c-means clustering algorithm,” *Journal of Jilin University (Science Edition)*, vol. 49, no. 6, pp. 1079–1086, 2011.